

**Safety and Integrity of  
Arctic Marine Pipelines**

**Progress Report #2  
Centrifuge Test PR3d-1 Report**

**Submitted to:**

**Minerals Management Service  
United States Department of the Interior  
Herndon, VA**

**Submitted by:**

**C-CORE  
St. John's, Newfoundland**

**C-CORE Publication 98-C2  
March, 1998**

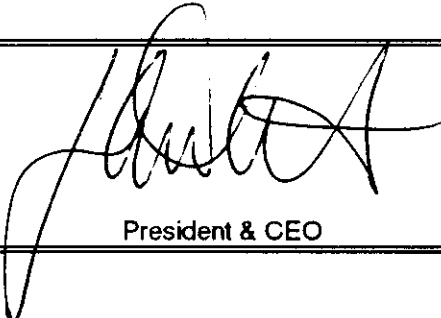


C-CORE  
Memorial University of Newfoundland  
St. John's, NF, A1B 3X5, Canada  
Tel. (709) 737-8354 Fax. (709) 737-4706

The correct citation for this report is :

Hurley, S., and Phillips, R. (1998). " Safety and Integrity of Arctic Marine Pipelines; Progress Report #2 - Centrifuge Test PR3d-1 Report." Contract Report for Minerals Management Service, United States Department of the Interior, C-CORE Publication 98-C2, March.

### QUALITY CONTROL REPORT

Clients:	Minerals Management Service United States Department of the Interior		
Project:			
Client's Contract Ref.:			
C-CORE Cost Center:	3-40425		
Document Title:	Safety and Integrity of Arctic Marine Pipelines Progress Report #2 - Centrifuge Test PR3d-1 Report		
C-CORE Pub. No.:	98-C2		
Prepared By:	Shawn Hurley, Ryan Phillips		
Date:	March, 1998		
Reviewers	Date	Document Accepted	Signature
Technical Accuracy	<i>9 Mar 98</i>		<i>Dave Wob</i>
	<i>MARCH 9<sup>TH</sup>, 1998</i>		<i>Mike Paulin</i>
Syntax	<i>March 9/98</i>		<i>Melissa Anselotti</i>
Layout & Presentation	<i>March 9/98</i>		<i>G. Jes Gitt</i>
General Evaluation			
Approval for Release			
Date:	<i>10 March / 98</i>		
	President & CEO		

## TABLE OF CONTENTS

1.0	INTRODUCTION .....	1
2.0	RESEARCH OBJECTIVES .....	3
3.0	MODEL PREPARATION .....	4
4.0	INSTRUMENTATION AND DATA ACQUISITION .....	7
5.0	CENTRIFUGE TEST PR3D-1 .....	8
	5.1 In-Flight Cone Penetration Test .....	8
	5.2 Model Scour Event .....	9
6.0	INVESTIGATION OF SOIL DEFORMATION .....	11
	6.1 Comparison to 1g Test Results .....	17
	6.1.1 Comparison of Sub-Scour Displacements .....	18
	6.1.2 Force Comparison .....	19
7.0	SUMMARY AND CONCLUSIONS .....	21
8.0	REFERENCES .....	22

## 1.0 INTRODUCTION

The Pressure Ridge Ice Scour Experiment (PRISE) is an ongoing jointly funded, international, multiphase program. The goal is to develop the capability to design pipelines and other seabed installations in regions scoured by ice, taking into account the soil deformations and stress changes within the soil which may be caused during a scouring event. The need for this capability was identified during a round-table discussion with several oil companies and federal government representatives in 1990 during an international workshop on ice scour held in Calgary.

Pipelines on Arctic seafloors in the U.S.A., Russia and Canada are in danger of being damaged by the action of sea ice pressure ridge keels that scour the seafloor. Sea ice forms during the long Arctic winters when the sea surface freezes. Storm winds during winter and early spring may put pressure on the 1-2m thick floating ice sheet, causing it to break and crush. This action creates linear mounds of piled-up ice blocks called pressure ridges; the keels of these pressure ridges may extend to 50 m below sea level. Ice scouring occurs when the pressure ridge keel touches, penetrates and continues to move forward through seabed soils at velocities of several centimetres per second. The scouring action typically creates curvilinear troughs, called scour marks, characterised by lateral mounds of soil created by the forward bulldozing action and lateral heaving induced by the scouring keel.

Oil and gas pipelines must be buried below the maximum expected scour depth to avoid direct ice/pipeline interaction which would cause serious damage to the pipe. However, just as soil at the seabed surface is subject to large scour-induced displacements, the soil beneath a scouring keel also moves. These sub-scour deformations also must be taken into account as they may cause unacceptable shear and bending stresses in a buried pipeline.

A safe burial depth must be selected to ensure pipeline safety and integrity in areas affected by ice scouring. The “safe” burial depth will not be the same for every region of the seafloor. This is dependant on three factors: (1) the maximum expected depth of ice-scouring, which will determine the absolute minimum top-of-pipe depth of burial; (2) the soil type and condition which will affect the response of sub-scour soils to ice induced stresses, and (3) the mechanism of load transfer from the deforming soil to the buried pipe. Thus the problem of pressure ridge ice scouring is, for each case, to determine a safe burial depth that not only will avoid direct ice/pipeline interaction, but also will minimize the risk of damage due to sub-scour soil movements.

This report presents the results of the first centrifuge test conducted as part of PRISE Phase 3d. The experiment was conducted at 1:10 scale thus centrifugal acceleration at the base of the model keel was set to 10g. The attack angle was 30° and the target scour depth was 7.5 mm. The model testbed was prepared using dry No. 00 silica sand with an average relative density of 64.1%.

## **2.0 RESEARCH OBJECTIVES**

The principal objective of the work being conducted for the MMS is to examine the magnitude and extent of sub-scour deformations in a dilatant soil. This information is essential to achieve the PRISE goal of designing pipelines and other seabed installations for regions scoured by ice, and to take into account the soil deformations and stress changes which may be caused during a scour event.

The objective will be achieved through four activities:

- (1) Direct field observation of sub-scour deformations under fresh ice scours in compact silt in a tidal estuary. This is documented in Paulin (1997).
- (2) Simulation of full scale or field ice scour events by two centrifuge modelling experiments;
- (3) Development of the existing numerical model to predict sub-scour deformation profiles in dilatant materials; and
- (4) Assistance in developing the MMS Alaskan workshop on indigenous knowledge in technology.

This work is being carried out as Phase 3d of PRISE.

This report addresses the first centrifuge modelling test of activity (2). Activity (4) has also been completed.

### 3.0 MODEL PREPARATION

It was originally proposed that the centrifuge modelling tests be conducted in a dilatant material, such as a compact silt, and the results compared to field (1g) results. However, due to the limited amount of 1g sub-scour deformation data in silt, due to the fact that field tests were conducted in frozen ground and due to the problems associated with obtaining similar geotechnical properties for silt between the model and full scale, it was decided to conduct the first test using the same "class" of material. Dense sand, like a compact silt, dilates when sheared. Since relevant full scale data are available for comparison, dense sand was used to prepare the first centrifuge model.

Model preparation began November 24/1997. The model seabed was prepared from dry No. 00 silica sand with the index properties listed in Table 1.

**Table 1. Index Properties of No. 00 Silica Sand**

Maximum dry density ( $\rho_d$ )	1595.3 kg/m <sup>3</sup>
Minimum dry density ( $\rho_d$ )	1312.5 kg/m <sup>3</sup>
Specific gravity ( $G_s$ )	2.68
Effective grain size ( $D_{10}$ )	0.132 mm
Mean grain size ( $D_{50}$ )	0.26 mm
Uniformity coefficient ( $C_u$ )	2.12

The sand was dry pluviated from a large hopper which was suspended over the strongbox. The mass flow rate of sand was controlled by a flow control valve plate at the hopper base release orifice. The dry density of the sand was periodically monitored during placement using small density cups. Relative density information is presented in Table 2. The average dry density and relative density ( $D_R$ ) were approximately 1480.8 kg/m<sup>3</sup> and 64.1% respectively.

Soil deformation markers were positioned at predetermined locations within the sand testbed during model preparation. Deformation markers consisting of a combination of blue sand and solder strand segments were placed in a straight line perpendicular to the scour direction at four and five scour depths below the bottom of the model keel. Measurements were taken along the length of the blue sand/solder strand segment to record its pre-test position. These deformation markers in the pre-test position are depicted in Figure 1. At the remaining positions, from three scour depths below the keel to the testbed surface, markers consisted of either 2.5 mm diameter lead shot balls or coloured 2 mm diameter plastic markers. The dry sand was levelled to the required elevation using a vacuum system and then the small round markers were carefully placed on the levelled sand surface. At each level (3 scour depths, 2 scour depths, 1 scour depth, 0.5 scour depths, scour elevation and the testbed surface) single strings of twelve markers each were placed in straight lines, approximately 20 mm apart, perpendicular to the scour direction. The X and Y coordinates of each marker were recorded relative to a fixed reference point on the strongbox. Figures 2 and 3 show deformation markers at one half, one, two and three scour depths below the bottom of the model keel. On the testbed surface, both lead shot and plastic markers were used since this was where the greatest deformation was expected to occur. These deformation markers, in their initial position, as well as deformation markers at the scour elevation are shown in Figure 4. Table 2 also lists the positions of the deformation markers relative to the base of the scouring model pressure ridge keel. In order to place the horizontal drive and model keel in its initial position, a channel with approximate dimensions of 10 cm by 10 cm and 1 cm deep was created at one end of the strongbox using the vacuum. The drive unit with the model keel attached was then lowered into position and secured to the strongbox.

**Table 2. Sand State at Placement and Deformation Marker Positions**

Measurement Position	Average Z <sup>1</sup> Elevation (mm)	Marker Type	Average $\rho_d$ (kg/m <sup>3</sup> )	Average $D_R$ (%)
5 scour depths below keel	184.2	Blue Sand/Solder Strand	1495.7	69.1
4 scour depths below keel	176.6	Blue Sand/Solder Strand	N/A	N/A
3 scour depths below keel	169.4	Lead Shot	1490.6	67.4
2 scour depths below keel	161.7	Lead Shot	1491.3	67.6
1 scour depth below keel	155.3	Lead Shot	1468.7	60.0
½ scour depth below keel	149.7	Coloured Markers	1463.3	58.1
Scour elevation	145.4	Lead Shot	1489.6	67.1
Surface elevation	138.2	Lead Shot/Coloured Markers	1466.6	59.3

1. Z measurements were taken from the top of the strongbox and are positive downwards.

#### 4.0 INSTRUMENTATION AND DATA ACQUISITION

Table 3 provides a summary of the instrumentation used in centrifuge test PR3d-1. In total, 14 active transducers were employed, including instrumentation used to measure the vertical and horizontal loads and contact pressures acting on the model keel and the keel position during the scour event. Figure 5 shows the locations of the transducers which were attached to the model keel.

**Table 3. Electronic Instrumentation**

Device	Identification	Measured or Derived Quantity
Tension Cell	TC04A	Model horizontal force
Tension Cell	TC04B	Model horizontal force
Load Cell	LC394469	Model vertical force / keel front
Load Cell	LC513034	Model vertical force / keel front
Load Cell	LC394580	Model vertical force / keel rear
Load Cell	LC490203	Model vertical force / keel rear
Pressure Transducer	PT423117	Contact pressure / horizontal base
Pressure Transducer	PT423107	Contact pressure / inclined surface
Pressure Transducer	PT517931	Contact pressure / inclined surface
Pressure Transducer	PT504863	Contact pressure / inclined surface
String Potentiometer	SP02	Model horizontal position
Displacement Transducer	LDT12	Sand surface settlement
CPT Load Cell	SANDCONE #2	Cone tip resistance
CPT Vertical Potentiometer	VDISPL	Cone vertical displacement

## **5.0 CENTRIFUGE TEST PR3D-1**

Centrifuge test PR3d-1 was conducted on December 2/1997. Figure 6 is a diagram of the experimental setup. To begin the test, the model was accelerated to 42 rpm which was equivalent to 10g at the base of the model keel. At this acceleration level, the model keel represented a prototype width of 1 m and a prototype scour depth of 75 mm. A linear displacement transducer (LDT) was employed to measure surface settlement and the output from the LDT is presented in Figure 7. Based on the LDT output, it can be seen that settlement of the sand testbed during acceleration to 10g was negligible.

### **5.1 In-Flight Cone Penetration Test**

Before conducting the scour, an in-flight cone penetrometer test (CPT) was performed. The CPT test gave an indication of the testbed conditions just prior to conducting the actual scour event. The cone tip employed had an angle of  $60^\circ$  with a cross sectional area of  $100 \text{ mm}^2$ . The penetration rate was 3.0 mm/sec and the total depth of penetration into the model was approximately 200 mm. The location of the cone penetrometer test is shown in Figure 6 and a plot of tip resistance with depth is presented in Figure 8.

## 5.2 Model Scour Event

The model conditions applicable to centrifuge test PR3d-1 may be summarised as follows:

Model Scale:	10:1
Scour Width:	100 mm
Scour Cut Depth:	7 mm (target 7.5 mm)
Attack Angle:	30°
Velocity:	100 mm/s
Material:	Dry No. 00 Silica sand

Data acquired during the scouring event included measurement of resultant forces and contact pressures acting on the model keel. The total horizontal force was computed through summation of contributions from individual tension load cells (TC04A and TC04B) located at the connection between the drive system pulling cables and the model keel. Figure 9 shows the measured horizontal force for each tension cell plotted against keel displacement during the scour event. Steady state conditions were achieved after about 300 mm of keel displacement. The total average horizontal force imposed under steady state conditions was approximately 0.142 kN at model scale (or 14.2 kN at prototype scale).

The total vertical force was evaluated through summation of the responses of the four tension/compression load cells (LC394469, LC513034, LC394580, and LC490203) which linked the model keel to the carriage assembly. Figure 10 shows the measured vertical force from each load cell, plotted against keel displacement during the scour event. The total average vertical force was approximately 0.162 kN (or 16.2 kN at prototype scale) which implied a vertical/horizontal force ratio of 1.14 for steady state conditions.

The contact pressures developed during the scouring event are displayed in Figure 11 which presents the data records for the four interface pressure transducers (PT423107, PT517931, PT423117, and PT504863) mounted on the model keel. The pressure record for the transducer located at the horizontal base of the keel indicated an average response over the duration of the event of 2.67 kPa. The two pressure transducers located on the lower positions of the inclined face of the keel displayed average responses of 60.8 and 50.2 kPa. The transducer located on the upper position of the inclined face exhibited a response of 17.8 kPa.

Figure 12 shows the keel displacement plotted versus time during the model scouring event, as determined from measurements of the string potentiometer (SP02) which was attached to the carriage assembly. This data record was used to evaluate the horizontal position of the model keel in presentation of the results for each of the other transducers. The actual keel velocity or scour rate was 106.1 mm/s, equal to the slope of the displacement-time curve.

## 6.0 INVESTIGATION OF SOIL DEFORMATION

Post-test investigation of the sand testbed included photographic documentation and visual inspection of scour morphology, profiling of the scoured surface, and examination of sub-scour effects through excavation, measurement and photography of the buried displacement markers. Photographs which display two different views of the model scour are presented in Figure 13. The sidewalls of the incision were characterised by a sharply sloping berm of material deposited from the frontal mound along the entire length of the scour rising to a maximum elevation on the order of 11 mm above the initial testbed elevation. A substantial frontal spoil mound was developed at the front of the keel, which rose to approximately 16 mm above the initial testbed surface.

Profiles of the deformed sand surface were acquired using C-CORE's laser profiling system. Cross-sectional profiles obtained at horizontal intervals of 50 mm along the scour length are presented in Figures 14 through 31, beginning at y-coordinate equal to 85 mm at the initial position of the model keel. From measurements taken after completion of the test (6.8 mm) and a review of the cross-sectional laser profiles, the average scour depth attained for the steady-state scouring condition was 7 mm or 70 mm at prototype scale.

After the post-test sand surface was photographed and profiled, the positions (X,Y,Z) of the displacement markers, which were clearly visible on the sand surface, were measured. These displacement markers were then removed and excavation with a vacuum system began to locate the remaining markers buried within the testbed. For each string of displacement markers, excavation with the vacuum system began at the marker furthest away from centreline of the scour. It was believed that these markers would have undergone the least amount of displacement and therefore

would be the easiest to locate. Table 4 presents the pre-test and post-test X and Y coordinates of each displacement marker as well as the computed X, Y and Z displacements.

**Table 4. Marker Displacements**

ID	X <sub>i</sub> (mm)	Y <sub>i</sub> (mm)	X <sub>r</sub> (mm)	Y <sub>r</sub> (mm)	ΔX (mm)	ΔY (mm)	ΔZ (mm)
SP <sup>1</sup> -1	360.0	455.5	359.0	456.0	1.0	0.5	0.0
SP-2	381.0	456.0	381.0	457.0	0.0	1.0	0.0
SP-3	400.0	456.0	395.5	459.0	4.5	3.0	-2.2
SP-4	420.0	456.5	410.0	465.0	10.0	8.5	-4.2
SP-5	441.0	456.5	387.0	528.0	54.0	71.5	-4.2
SP-6	461.0	457.0	402.0	630.0	59.0	173.0	-9.2
SP-7	482.0	458.0	542.0	644.0	-60.0	186.0	-11.2
SP-8	502.5	460.0	556.0	543.0	-53.5	83.0	-2.2
SP-9	519.0	460.0	536.5	481.0	-17.5	21.0	-7.2
SP-10	540.0	460.0	540.0	461.0	0.0	1.0	0.0
SP-11	561.0	461.0	563.0	464.0	-2.0	3.0	0.0
SP-12	581.0	461.0	582.0	464.0	-1.0	3.0	0.0
SL <sup>2</sup> -1	360.0	560.0	362.0	560.0	-2.0	0.0	0.0
SL-2	380.0	560.0	382.0	560.0	-2.0	0.0	0.0
SL-3	403.0	559.5	402.0	562.0	1.0	2.5	-2.2
SL-4	420.0	559.5	415.0	568.0	5.0	8.5	-4.2
SL-5	441.5	559.0	410.0	634.0	31.5	75.0	-8.2
SL-6	460.0	560.0	401.0	723.0	59.0	163.0	-3.2
SL-7	480.0	560.0	509.0	940.0	-29.0	380.0	-10.0
SL-8	500.0	561.5	546.0	755.0	-46.0	193.5	-3.2
SL-9	521.0	562.0	539.0	634.0	-18.0	72.0	-10.2
SL-10	541.0	562.0	541.0	561.5	0.0	-0.5	-2.2

ID	X <sub>i</sub> (mm)	Y <sub>i</sub> (mm)	X <sub>r</sub> (mm)	Y <sub>r</sub> (mm)	ΔX (mm)	ΔY (mm)	ΔZ (mm)
SL-11	561.0	560.0	563.0	560.0	-2.0	0.0	0.0
SL-12	580.0	561.0	581.0	561.0	-1.0	0.0	0.0
SC <sup>3</sup> -1	360.0	531.0	360.0	531.0	0.0	0.0	0.0
SC-2	380.0	530.0	380.0	530.0	0.0	0.0	0.0
SC-3	400.0	530.0	400.0	530.0	0.0	0.0	0.0
SC-4	420.0	530.0	418.0	535.0	2.0	5.0	-2.4
SC-5	440.0	530.0	425.0	645.0	15.0	115.0	-1.4
SC-6	460.5	530.0	398.0	726.0	62.5	196.0	-9.4
SC-7	480.0	529.0	532.0	578.0	-52.0	49.0	-11.4
SC-8	499.0	530.0	503.0	585.0	-4.0	55.0	-5.0
SC-9	520.0	530.0	522.0	542.0	-2.0	12.0	-4.4
SC-10	540.0	529.0	540.0	526.0	0.0	-3.0	-1.4
SC-11	561.0	529.0	559.0	525.0	2.0	-4.0	-1.4
SC-12	580.0	529.0	580.0	525.0	0.0	-4.0	0.0
SC05 <sup>4</sup> -1	356.0	505.0	358.0	505.0	-2.0	0.0	-0.7
SC05-2	377.0	505.0	379.0	504.0	-2.0	-1.0	0.0
SC05-3	400.0	504.0	400.0	502.0	0.0	-2.0	-0.7
SC05-4	419.0	505.0	419.0	505.0	0.0	0.0	-0.7
SC05-5	440.0	503.5	439.0	516.0	1.0	12.5	-0.7
SC05-6	459.0	503.0	456.0	524.0	3.0	21.0	-1.7
SC05-7	479.5	504.0	476.0	522.0	3.5	18.0	-1.7
SC05-8	501.0	504.0	499.0	506.0	2.0	2.0	-0.7
SC05-9	520.0	504.0	521.0	505.0	-1.0	1.0	-0.7
SC05-10	539.0	504.0	540.0	503.5	-1.0	-0.5	-0.7
SC05-11	562.0	504.5	560.0	504.0	2.0	-0.5	-0.7

ID	X <sub>i</sub> (mm)	Y <sub>i</sub> (mm)	X <sub>r</sub> (mm)	Y <sub>r</sub> (mm)	ΔX (mm)	ΔY (mm)	ΔZ (mm)
SC05-12	579.0	504.0	579.0	504.0	0.0	0.0	-0.7
SC1 <sup>5</sup> -1	360.0	504.0	360.0	504.0	0.0	0.0	1.0
SC1-2	379.0	503.0	378.0	503.0	1.0	0.0	1.0
SC1-3	400.0	503.0	398.0	504.0	2.0	1.0	1.0
SC1-4	419.5	503.5	417.0	504.0	2.5	0.5	1.0
SC1-5	439.0	502.5	435.0	504.0	4.0	1.5	1.0
SC1-6	458.0	503.5	455.0	508.0	3.0	4.5	1.0
SC1-7	478.0	503.0	475.0	505.5	3.0	2.5	1.0
SC1-8	499.0	505.0	495.0	506.0	4.0	1.0	1.0
SC1-9	519.0	504.0	520.0	505.0	-1.0	1.0	1.0
SC1-10	539.0	504.0	540.0	505.0	-1.0	1.0	1.0
SC1-11	559.0	504.0	559.0	505.0	0.0	1.0	1.0
SC1-12	581.0	503.0	580.0	504.0	1.0	1.0	0.0
SC2-1	356.5	602.0	358.0	601.0	-1.5	-1.0	0.0
SC2-2	377.0	602.5	378.0	602.0	-1.0	-0.5	0.0
SC2-3	396.0	602.5	398.0	601.0	-2.0	-1.5	0.0
SC2-4	416.0	602.0	418.0	603.0	-2.0	1.0	0.0
SC2-5	435.0	601.0	436.0	603.0	-1.0	2.0	0.0
SC2-6	456.0	601.0	458.0	602.0	-2.0	1.0	0.0
SC2-7	477.0	601.5	478.0	602.0	-1.0	0.5	0.0
SC2-8	495.0	601.0	497.0	602.0	-2.0	1.0	0.0
SC2-9	517.0	603.0	517.0	602.5	0.0	-0.5	0.0
SC2-10	540.0	600.5	538.0	603.0	2.0	2.5	0.0
SC2-11	556.0	599.0	555.0	602.0	1.0	3.0	0.0
SC2-12	575.0	599.0	573.0	601.0	2.0	2.0	0.0

ID	X <sub>i</sub> (mm)	Y <sub>i</sub> (mm)	X <sub>r</sub> (mm)	Y <sub>r</sub> (mm)	ΔX (mm)	ΔY (mm)	ΔZ (mm)
SC3-1	360.0	600.0	361.0	599.0	-1.0	-1.0	0.0
SC3-2	378.0	600.0	377.0	600.0	1.0	0.0	0.0
SC3-3	400.0	599.5	398.0	600.0	2.0	0.5	0.0
SC3-4	418.0	598.0	418.0	600.0	0.0	2.0	0.0
SC3-5	438.0	599.0	435.0	600.0	3.0	1.0	0.0
SC3-6	459.0	599.0	457.0	600.5	2.0	1.5	0.0
SC3-7	479.0	600.0	478.0	601.0	1.0	1.0	0.0
SC3-8	497.5	601.0	500.0	600.0	-2.5	-1.0	0.0
SC3-9	516.0	600.0	519.0	600.0	-3.0	0.0	0.0
SC3-10	537.0	598.5	540.0	599.0	-3.0	0.5	0.0
SC3-11	556.0	600.0	560.0	600.0	-4.0	0.0	0.0
SC3-12	577.0	600.0	580.0	599.0	-3.0	-1.0	0.0
BS4 <sup>6</sup> -1	345.0	520.0	345.0	520.0	0.0	0.0	0.0
BS4-2	400.0	520.0	400.0	522.0	0.0	2.0	0.0
BS4-3	450.0	522.0	450.0	521.0	0.0	-1.0	0.0
BS4-4	500.0	521.0	500.0	521.0	0.0	0.0	0.0
BS4-5	550.0	520.0	550.0	522.0	0.0	2.0	0.0
BS4-6	600.0	516.0	600.0	518.0	0.0	2.0	0.0
SS4 <sup>7</sup> -1	364.0	781.0	364.0	780.0	0.0	-1.0	0.0
SS4-2	400.0	784.0	400.0	779.0	0.0	-5.0	0.0
SS4-3	450.0	780.0	450.0	779.0	0.0	-1.0	0.0
SS4-4	500.0	785.0	500.0	784.0	0.0	-1.0	0.0
SS4-5	550.0	785.0	550.0	785.0	0.0	0.0	0.0
SS4-6	574.0	785.0	574.0	787.0	0.0	2.0	0.0
BS5-1	350.0	510.0	350.0	506.0	0.0	-4.0	0.0

ID	X <sub>i</sub> (mm)	Y <sub>i</sub> (mm)	X <sub>r</sub> (mm)	Y <sub>r</sub> (mm)	ΔX (mm)	ΔY (mm)	ΔZ (mm)
BS5-2	400.0	505.0	400.0	505.0	0.0	0.0	0.0
BS5-3	450.0	507.0	450.0	507.0	0.0	0.0	0.0
BS5-4	500.0	512.0	500.0	510.0	0.0	-2.0	0.0
BS5-5	550.0	508.0	550.0	510.0	0.0	2.0	0.0
BS5-6	590.0	505.0	590.0	513.0	0.0	8.0	0.0
SS5-1	364.0	783.0	364.0	785.0	0.0	2.0	0.0
SS5-2	400.0	781.0	400.0	783.0	0.0	2.0	0.0
SS5-3	450.0	780.0	450.0	784.0	0.0	4.0	0.0
SS5-4	500.0	780.0	500.0	784.0	0.0	4.0	0.0
SS5-5	550.0	784.0	550.0	790.0	0.0	6.0	0.0
SS5-6	571.0	785.0	571.0	790.0	0.0	5.0	0.0

- Notes:
1. SP = Surface, plastic deformation marker
  2. SL = Surface, lead shot deformation marker
  3. SC = Scour elevation
  4. SC05 = One half a scour depth below bottom of model keel
  5. SC# = # represents # of scour depths below bottom of model keel
  6. BS# = Blue sand, # represents # of scour depths below bottom of model keel
  7. SS# = Solder strand, # represents # of scour depths below bottom of model keel

Table 4 indicates that only the deformation markers positioned up to one-half a scour depth below the model keel underwent significant displacement. At one scour depth, there was minimal displacement (4.5 mm in scour direction) of marker SC1-6 which was located close to the centreline of the scour. The greatest displacement occurred at the surface with a lead shot marker designated as SL-7 being displaced a total of 380.0 mm in the scour direction (+Y direction). This marker was also originally located close to the scour centreline. At the scour elevation, a maximum of 196 mm of displacement in the direction of scour was measured in marker SC-6. The deformation markers located furthest away from the scouring keel (close to the outside of the marker string) did not move

or underwent minimal displacement. Lateral displacement (in the X direction) of a deformation marker is mainly attributable to the marker being displaced or pushed to the side by the developing sand berm. The blue sand and solder strand located at four and five scour depths were unaffected by the passage of the keel. Although Table 4 indicates that these markers may have undergone some displacement, the differences in pre- and post-test positions can be attributed to slight disturbance during vacuum excavation of the sand around the markers. There was no evidence of disturbance to any of the round plastic or lead markers. It is believed that the displacement measurements given in Table 4 are accurate to within  $\pm 2$  mm.

Vector diagrams which depict the displacement of the markers located at the surface and scour elevation are given in Figure 32. Figure 33 is a plot of displacement versus depth below sand surface for displacement markers located close to the scour centerline.

### **6.1 Comparison to 1g Test Results**

Several 1g scour experiments have been performed by C-CORE in the sand scour tank in the laboratories of the Faculty of Engineering and Applied Science at the Memorial University of Newfoundland. Centrifuge test PR3d-1 was designed to model certain aspects of Test 3 and Test 4 conducted by Poorooshasb (1989). The relevant parameters of these tests are given in Table 5 while Table 6 lists the index properties of the sand used in the 1g experiments.

**Table 5. Poorooshab (1989) Test Parameters**

Parameter	Test 3	Test 4
Scour Width (mm)	860	860
Scour Depth (mm)	75	75
Attack Angle	30°	15°
Velocity (mm/s)	71	66
Material	Dry No. 0 Silica Sand	Dry No. 0 Silica Sand
Sand Relative Density ( $D_R$ ) (dense portion of testbed)	51%	64.4%

**Table 6. Index Properties of No. 0 Silica Sand**

Maximum dry density ( $\rho_d$ )	1665 kg/m <sup>3</sup>
Minimum dry density ( $\rho_d$ )	1378 kg/m <sup>3</sup>
Specific gravity ( $G_s$ )	2.69
Effective grain size ( $D_{10}$ )	0.170 mm
Mean grain size ( $D_{50}$ )	0.205 mm
Uniformity coefficient ( $C_u$ )	1.609

### 6.1.1 Comparison of Sub-Scour Displacements

Deformation markers for the 1g experiments consisted of engraved ball bearings and solder strands. A three dimensional pointer system was used to record pre- and post-test positions of deformation markers and reportedly had an accuracy of  $\pm 5$  mm. Figure 34 presents a comparison between sub-scour deformation data for the 1g experiments and the prototype sub-scour deformations from the centrifuge experiment for markers located close to the scour centerline. It can be seen that there is reasonably good agreement between centrifuge results and the 1g results. For both the centrifuge and 1g tests, sub-scour deformation occurs down to approximately one scour depth, below which

there is very little, if any, sub-scour deformation. Figure 35 is a vector diagram which compares significant horizontal ball bearing displacements measured during the centrifuge test with displacements measured by Poorooshab (1989). The displacements recorded by Poorooshab (1989) are displacements measured in ball bearings originally located in dense sand and close to or slightly above the scour elevation. The prototype scale centrifuge displacements (marker CF#) were measured in lead shot displacement markers located on the sand surface.

### 6.1.2 Force Comparison

In comparing scour force data, two non-dimensional numbers are used. These are vertical to horizontal force ratio and the normalized horizontal scour force. Horizontal scour force is a function of the sand density, the scour width, the scour depth, and the keel attack angle and is normalized using the same method as that outlined in PRISE (1995).

Table 7 presents the measured average vertical and horizontal dense sand forces, per unit keel width, from Poorooshab (1989), the prototype scale vertical and horizontal forces per unit width from the centrifuge test, and the vertical to horizontal force ratios.

**Table 7. Force Comparison**

Parameter	Test #3	Test #4	Centrifuge Test
Avg. vertical force ( $F_v$ ) per meter (kN/m)	6.98	11.63	16.2
Avg. horizontal force ( $F_h$ ) per meter (kN/m)	7.56	9.88	14.2
Force ratio ( $F_v / F_h$ )	0.92	1.18	1.14

The prototype vertical and horizontal forces measured during the centrifuge test are higher than those measured by Poorooshab (1989) but the ratio of vertical to horizontal forces is consistent. The discrepancy between forces can be attributed to the fact that a coarser sand was used during the 1g experiments, the prototype keel width for the centrifuge experiments was slightly larger than the 1g experiments (1 m as opposed to 0.86 m) and it might have been expected that the sand density would vary more over the area of the 1g testbed than the centrifuge strongbox. Another important difference is that the bottom and the attack face of the centrifuge keel were roughened whereas the bottom and the attack face of the 1g keel were smooth.

Figure 36 presents normalized horizontal force plotted against prototype scale scour depth for the centrifuge test, previous PRISE centrifuge tests conducted in loose and dense sand, the Poorooshab (1989) 1g tests, and Paulin's (1992) 1g tests, which were conducted in submerged No. 00 silica sand at a scour depth of 40 mm. It can be seen that the normalized horizontal forces are again higher than those measured by Poorooshab (1989) but are between the limits set by the 1g experiments of Poorooshab (1989) and Paulin (1992).

The vertical and horizontal forces measured during the centrifuge test had a cyclic component which was also observed by Poorooshab (1989), Paulin (1992) and during the PRISE (1995) centrifuge tests.

## 7.0 SUMMARY AND CONCLUSIONS

The first centrifuge test of PRISE Phase 3d was conducted in a dry dilatant material, namely a dense No. 00 Silica sand, and the results compared to a field event. It was decided to conduct the first test in a sand rather than a compact silt material due to the limited amount of 1g data for sub-scour deformations in silt, the fact that during the field experiments the ground was partially frozen and the difficulty in preparing a pure silt material.

The testbed for centrifuge test PR3d-1 consisted of dry No. 00 Silica sand. The results of this test were compared to 1g experiments also conducted by C-CORE. The main differences between the 10g test and the 1g tests were in attack angle (Test 4 = 15°), the type of sand used, the prototype scour width and the friction factor between keel contact surface and testbed sand.

In terms of sub-scour displacements, the results are very similar. The centrifuge data indicate that sub-scour deformation of the testbed material occurs down to about one scour depth. Below this depth, there is little or no displacement. The results of the 1g event indicate that sub-scour deformation was also observed down to about one scour depth below the bottom of the scouring model keel.

The measured prototype forces from the centrifuge test were somewhat higher than those measured during the 1g tests conducted by Poorooshasb (1989). The discrepancy is mainly attributable to the fact that different sand was used and there was a different friction factor between keel contact surface and the testbed sand.

## 8.0 REFERENCES

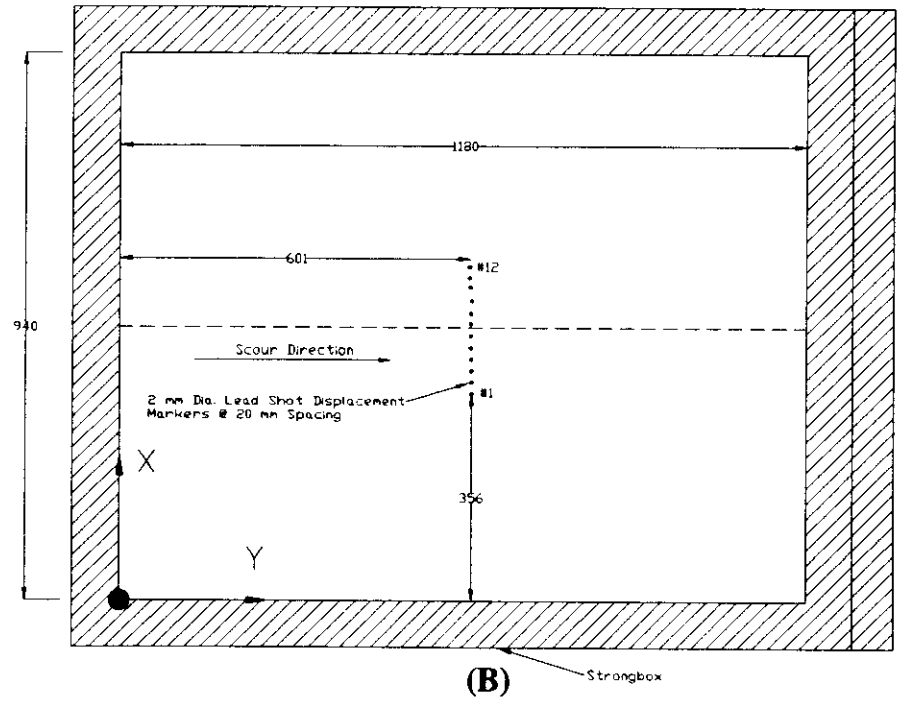
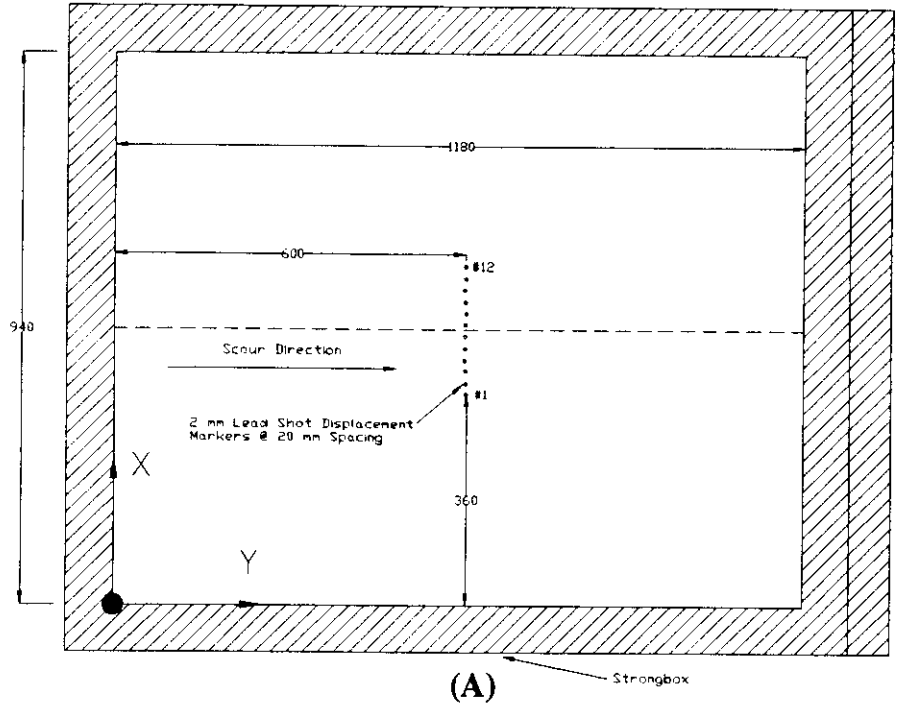
Paulin, M.J. (1992). "Physical Model Analysis of Iceberg Scour in Dry and Submerged Sand." M.Eng. Thesis, Faculty of Engineering and Applied Science, Memorial University of Newfoundland, St. John's, NF.

Paulin, M.J. (1997). "Safety and Integrity of Arctic Marine Pipelines; Progress Report #1 - Results of Field Study". Contract Report for Minerals Management Service, United States Department of the Interior, C-CORE Publication 97-C30, July.

Poorooshasb, F. (1989). "Large Scale Laboratory Tests of Seabed Scour". Contract Report for Fleet Technology Ltd., C-CORE Contract Number 89-C15.

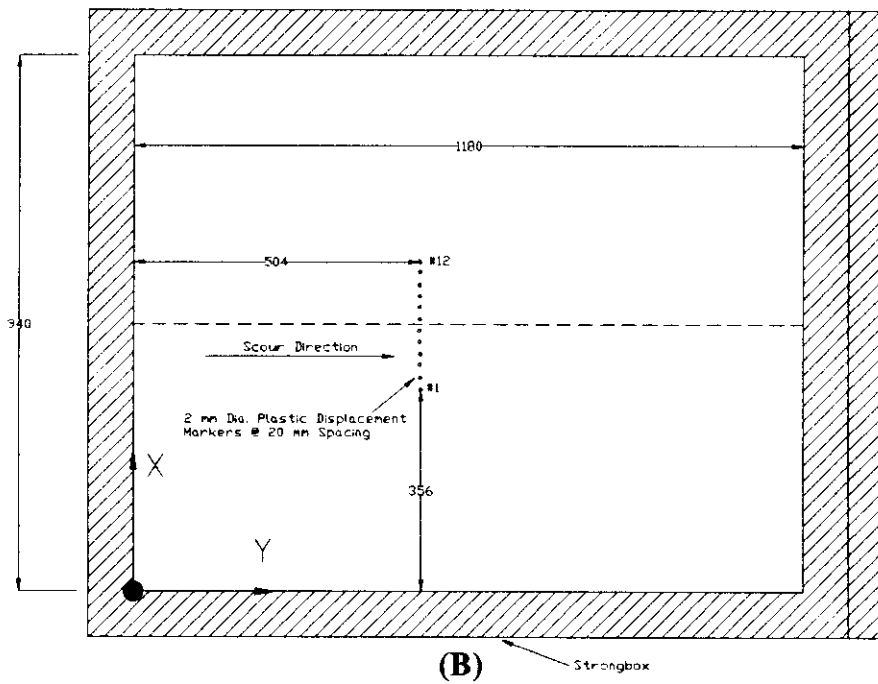
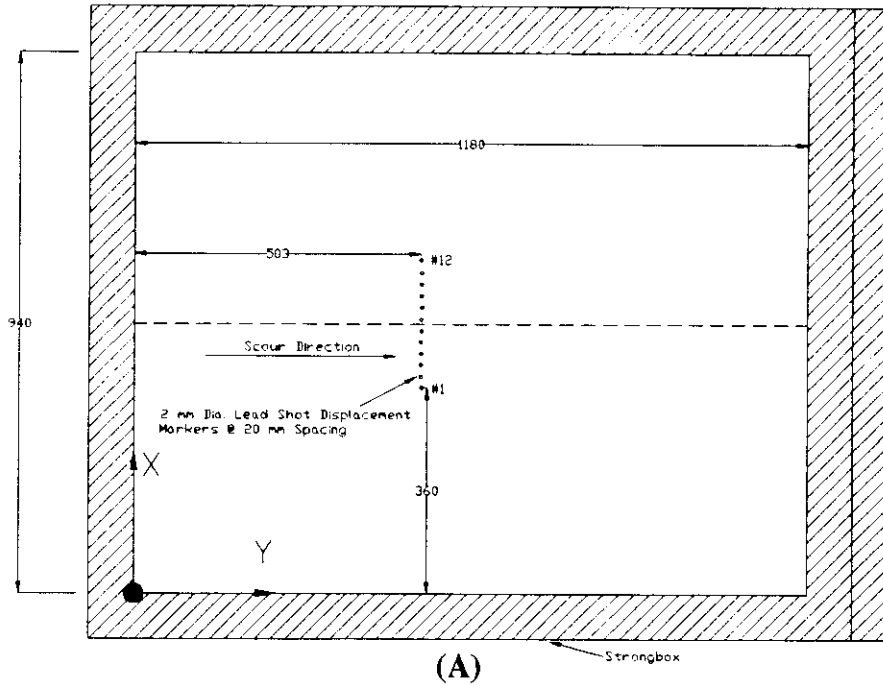
Pressure Ridge Ice Scour Experiment (PRISE) Phase 3: Centrifuge Modelling of Ice Keel Scour: Draft Final Report. April 1995.



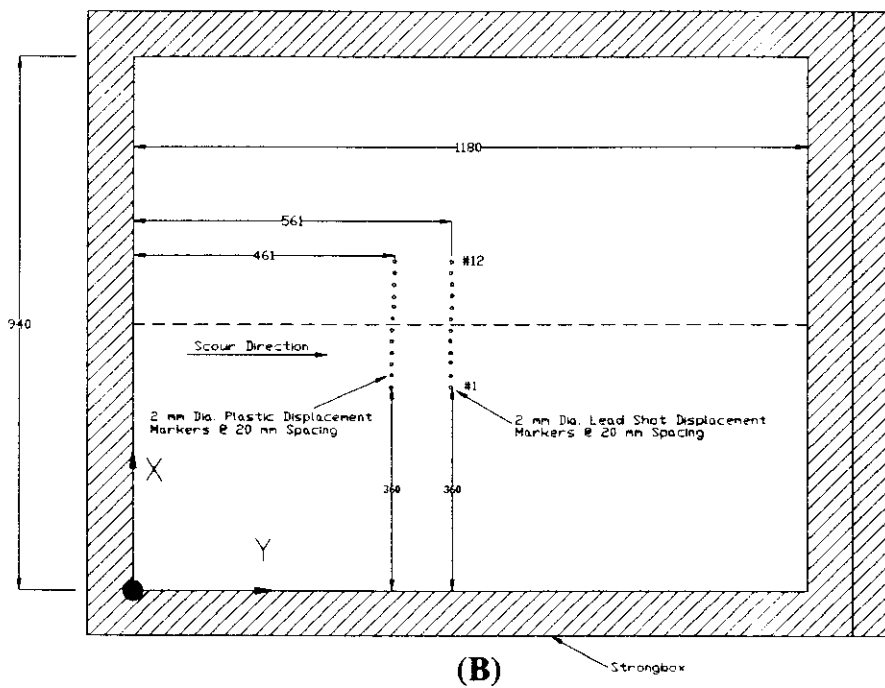
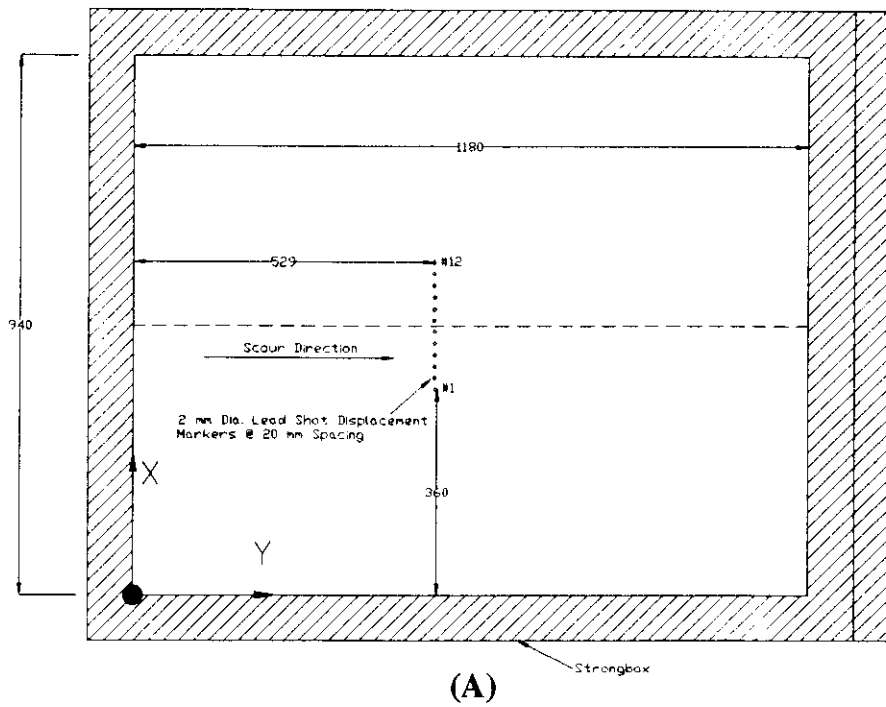


A) Deformation Markers at Three Scour Depths  
 B) Deformation Markers at Two Scour Depths

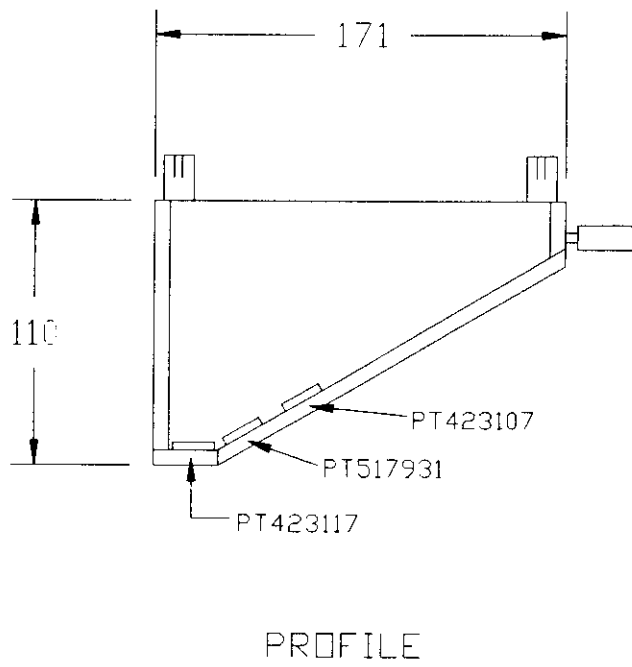
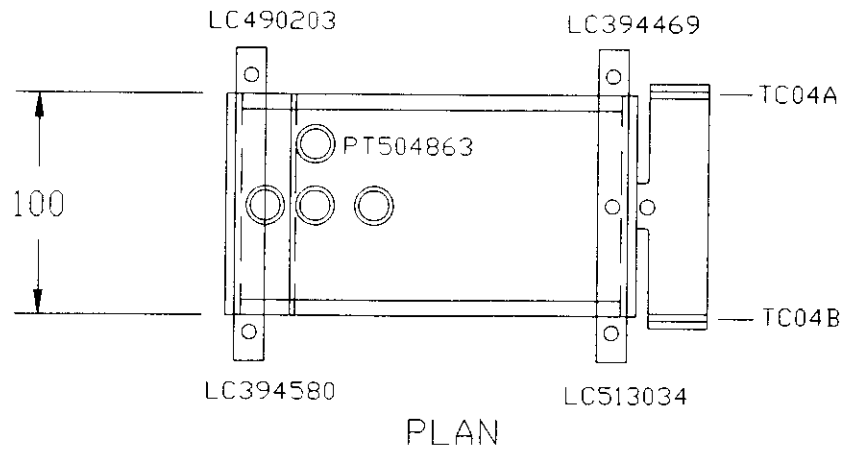




A) Deformation Markers at One Scour Depth  
 B) Deformation Markers at One Half a Scour Depth

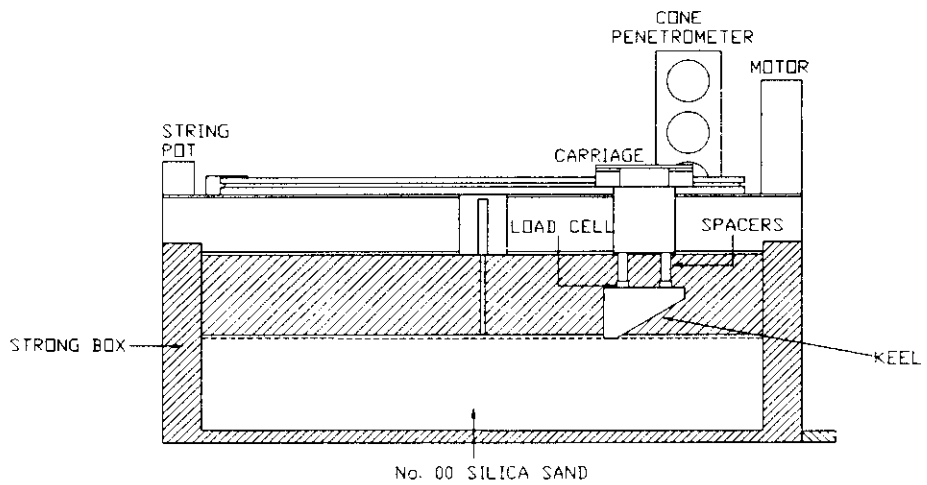
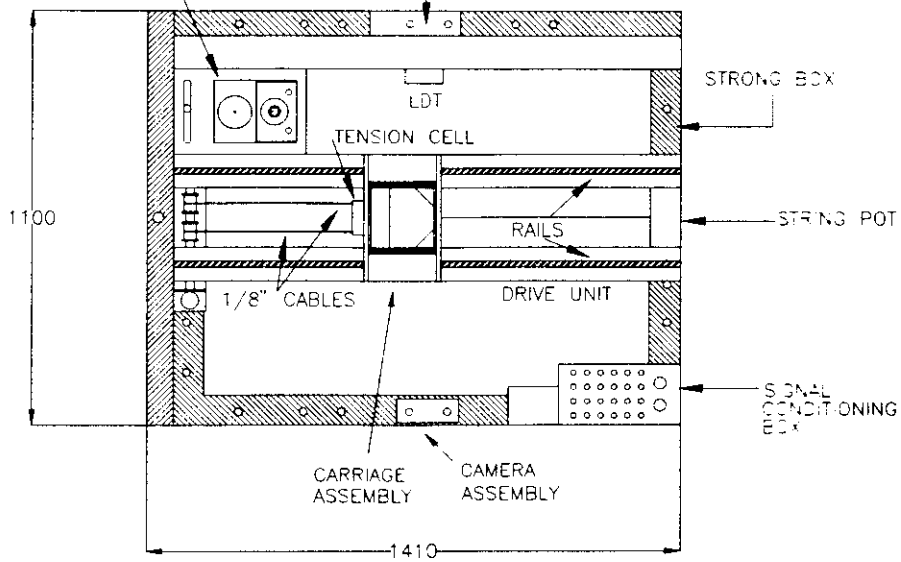


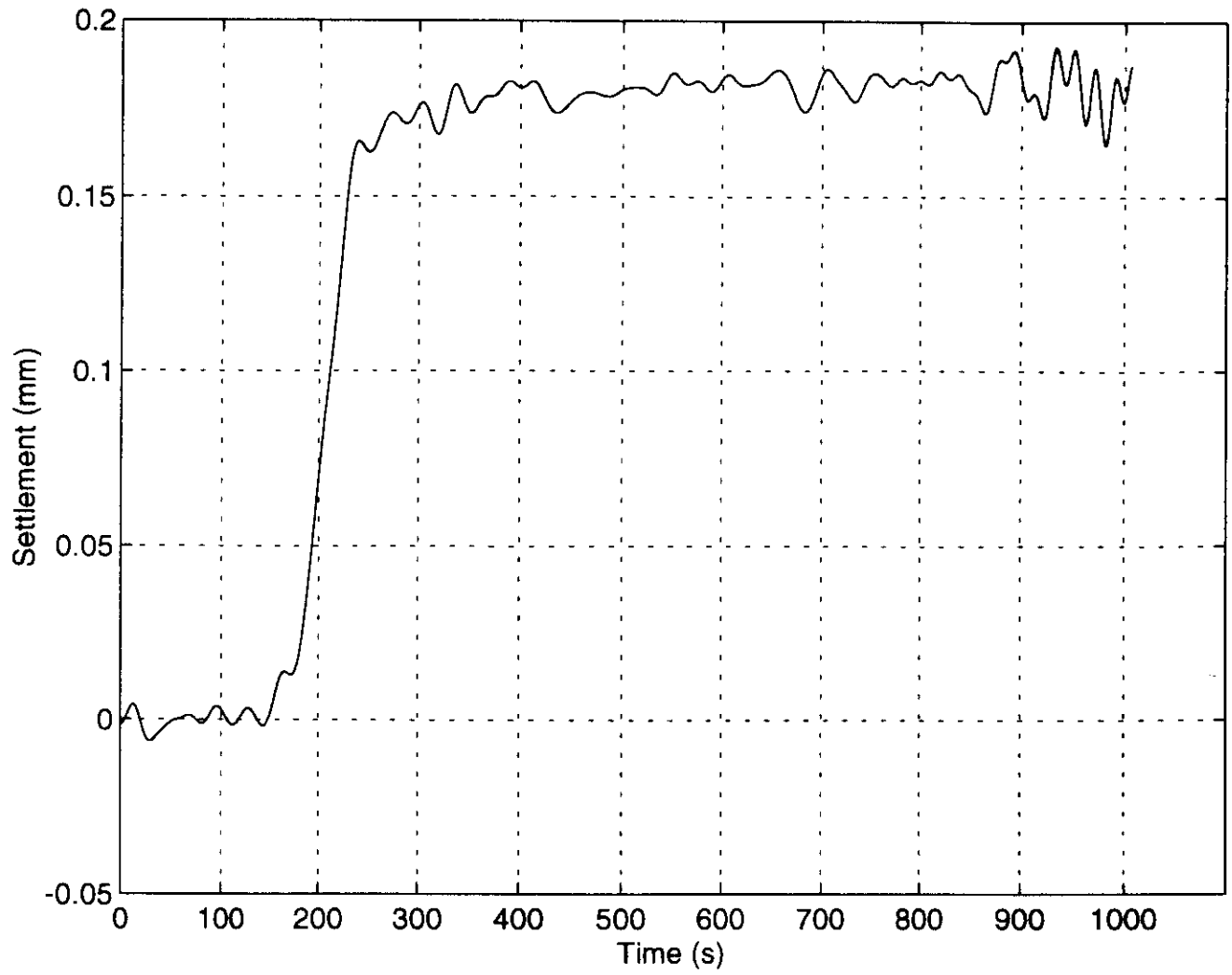
A) Deformation Markers at Scour Elevation  
 B) Deformation Markers on Testbed Surface



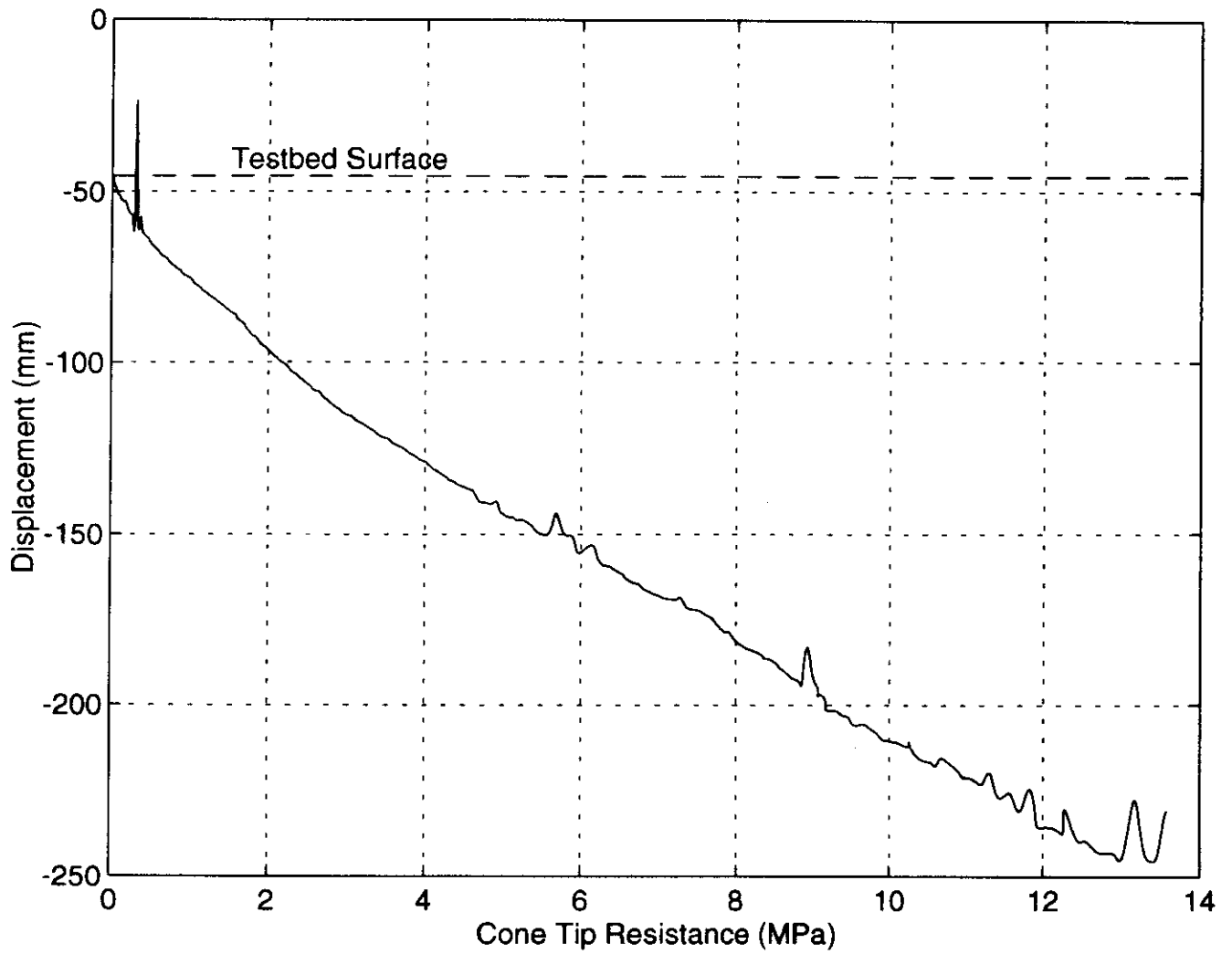
CONE PENETROMETER AND ACTUATOR

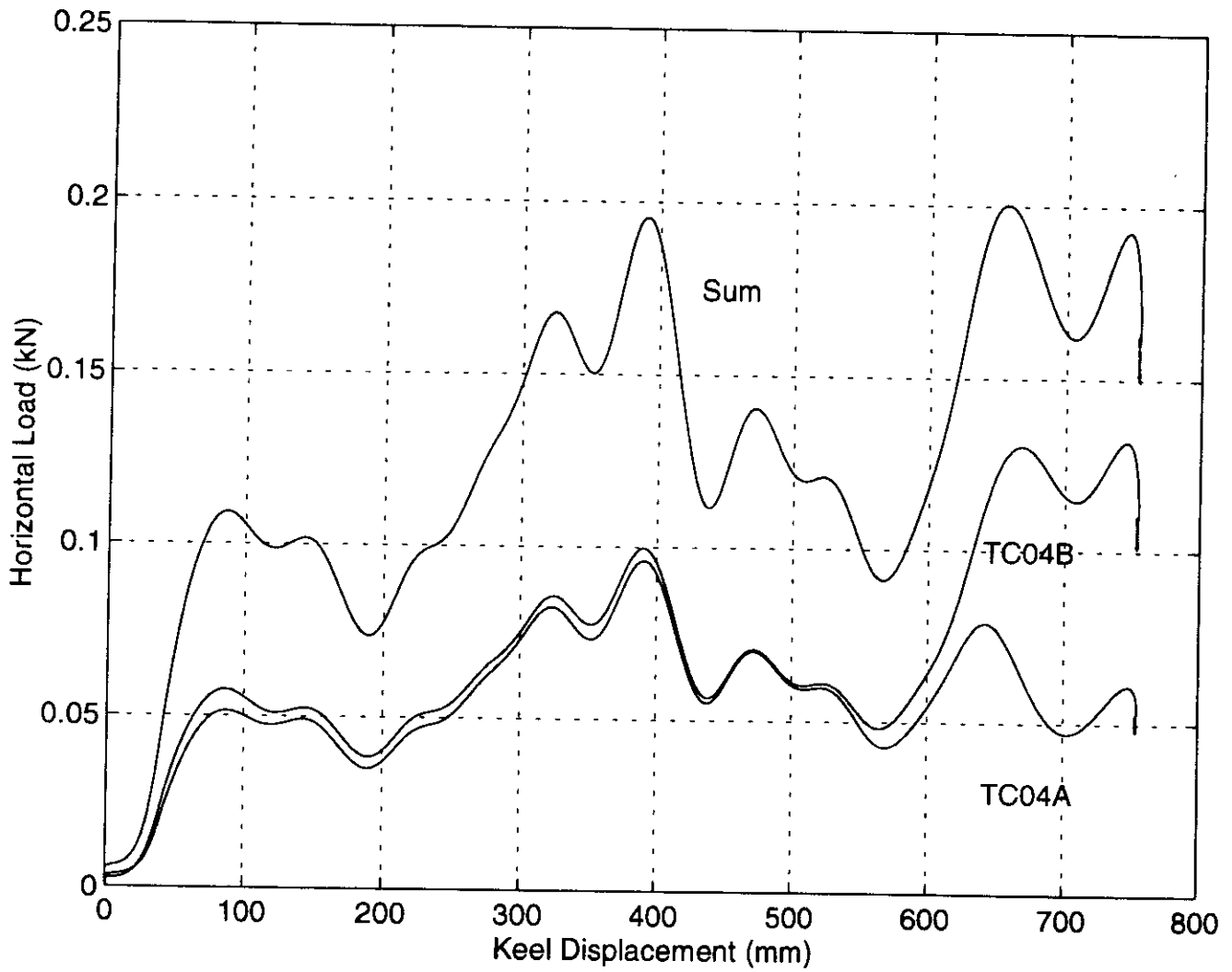
PATCH PANEL

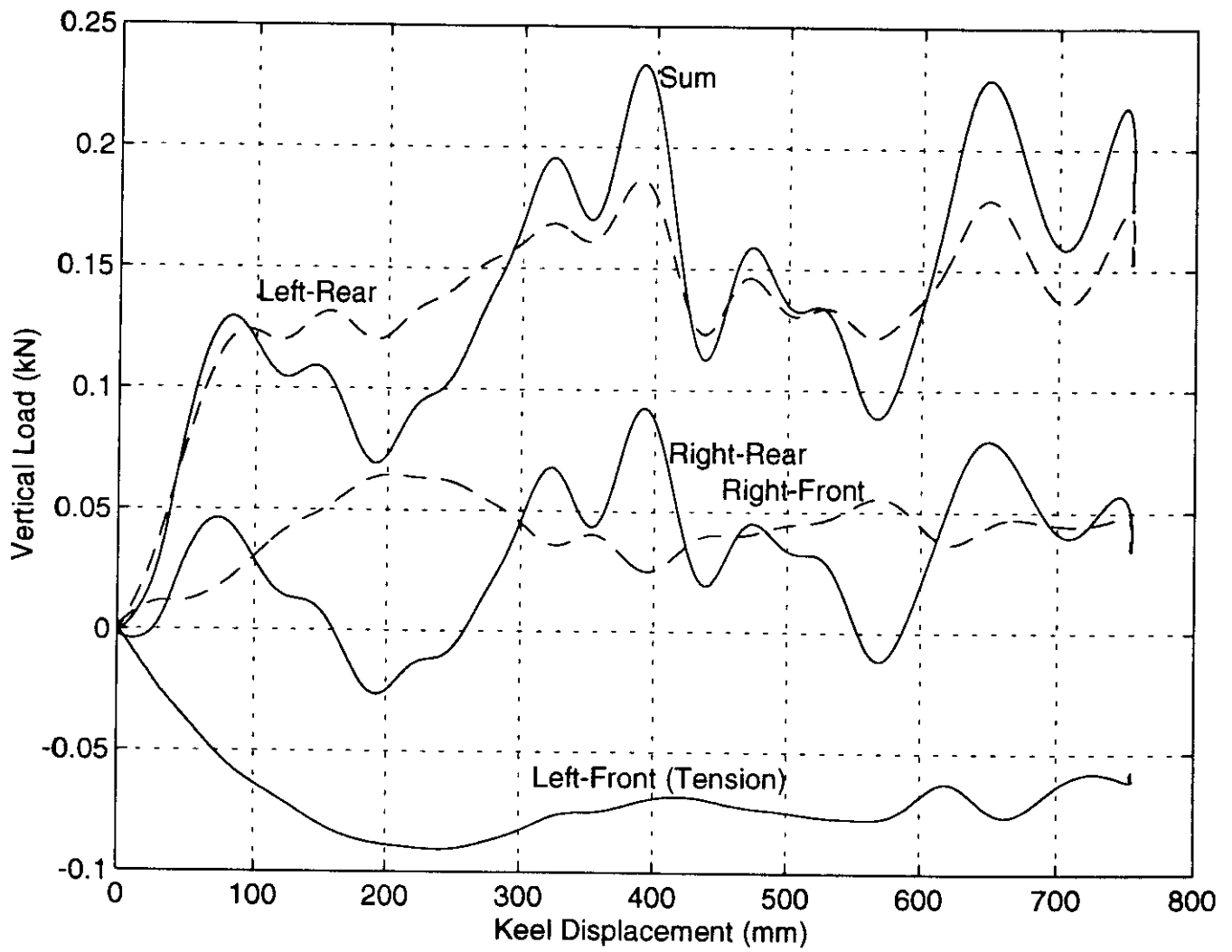


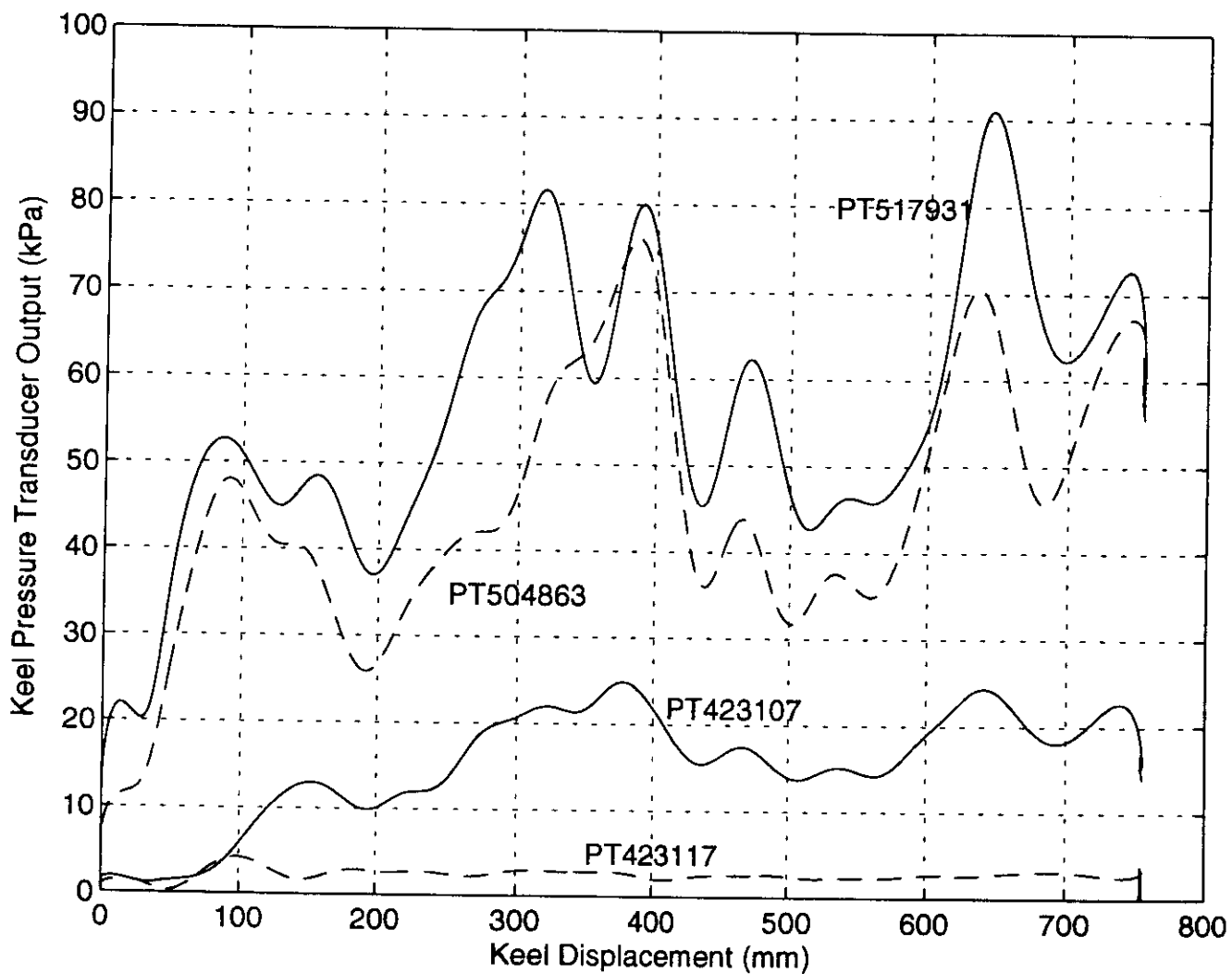


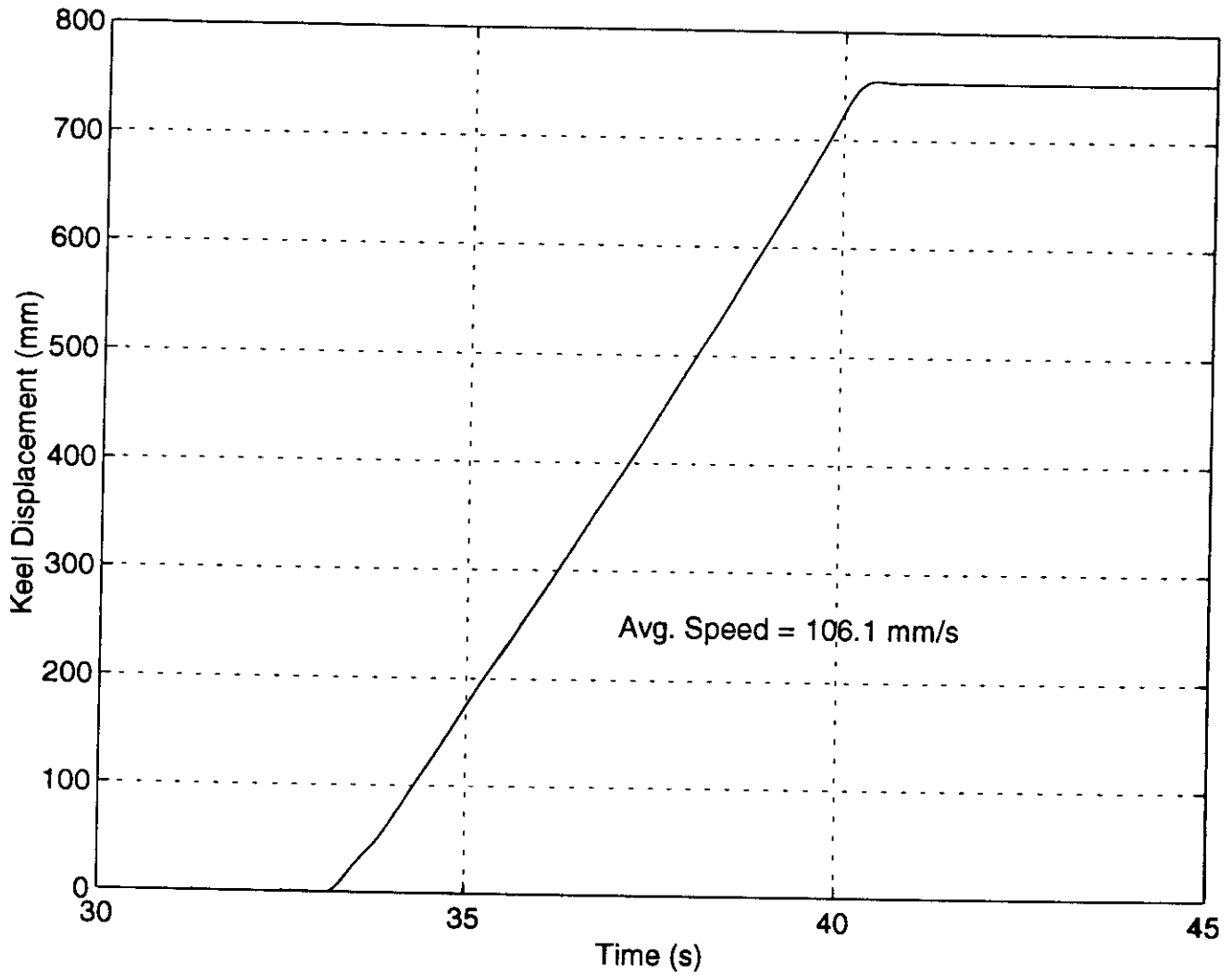
Linear Displacement Transducer (LDT) Output

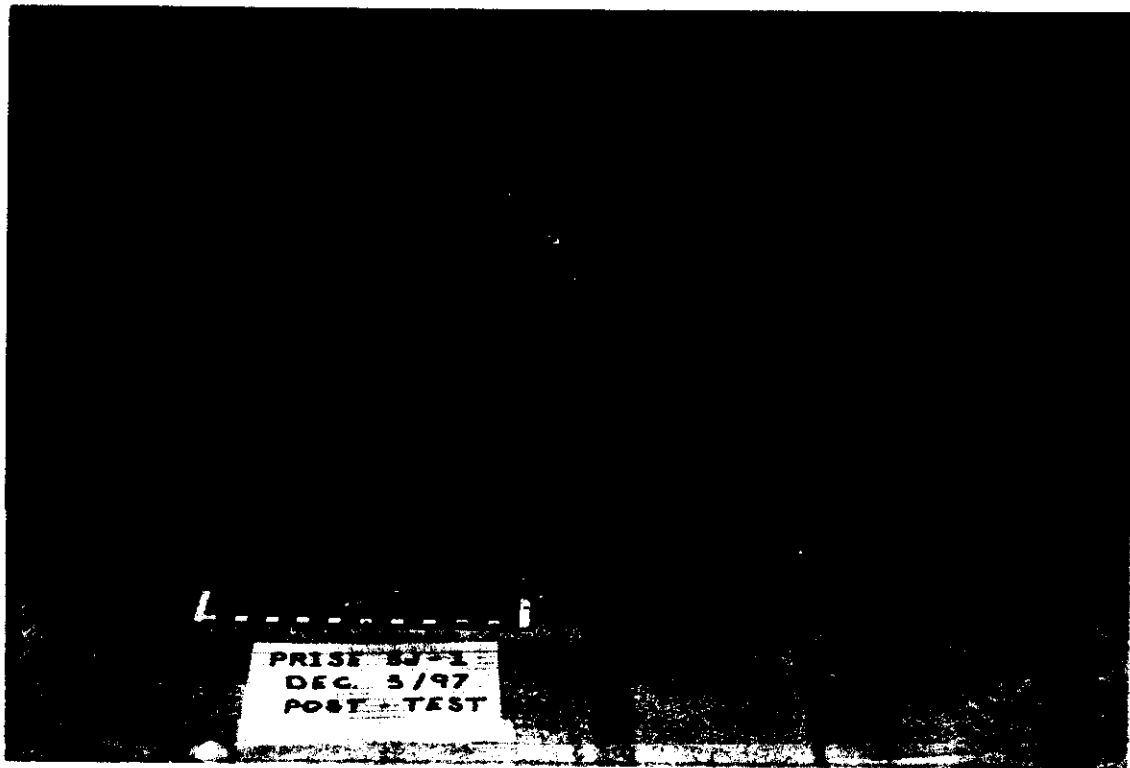
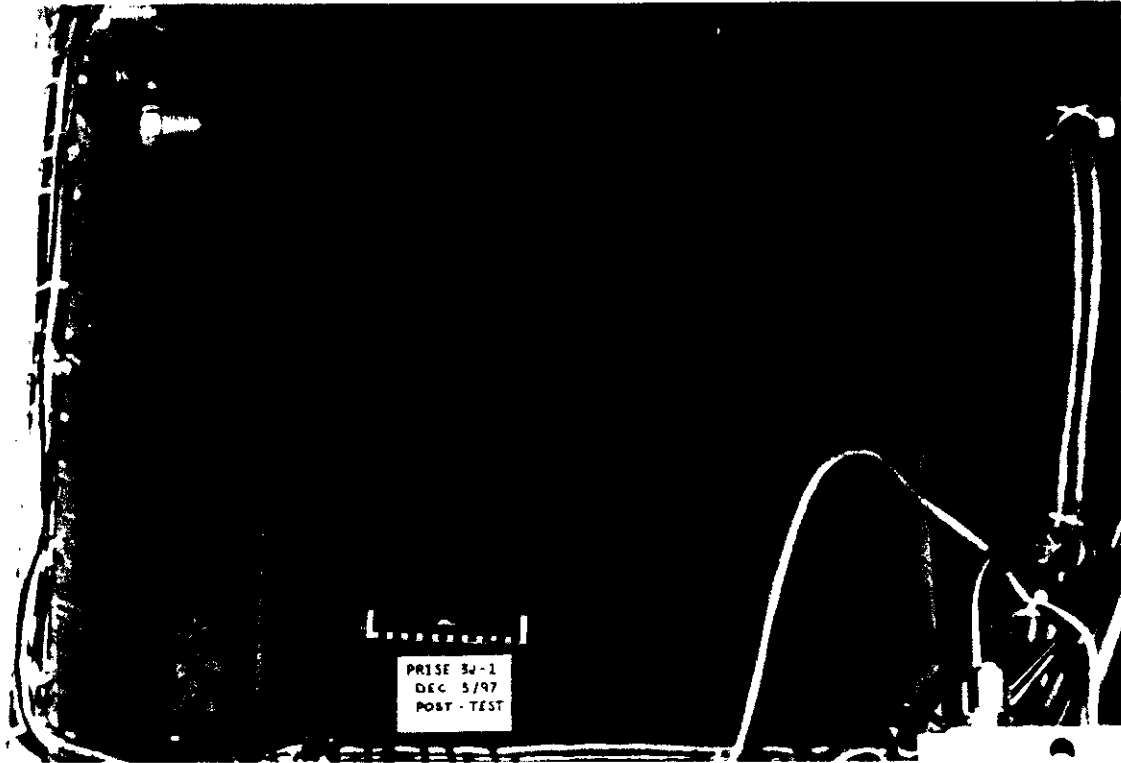


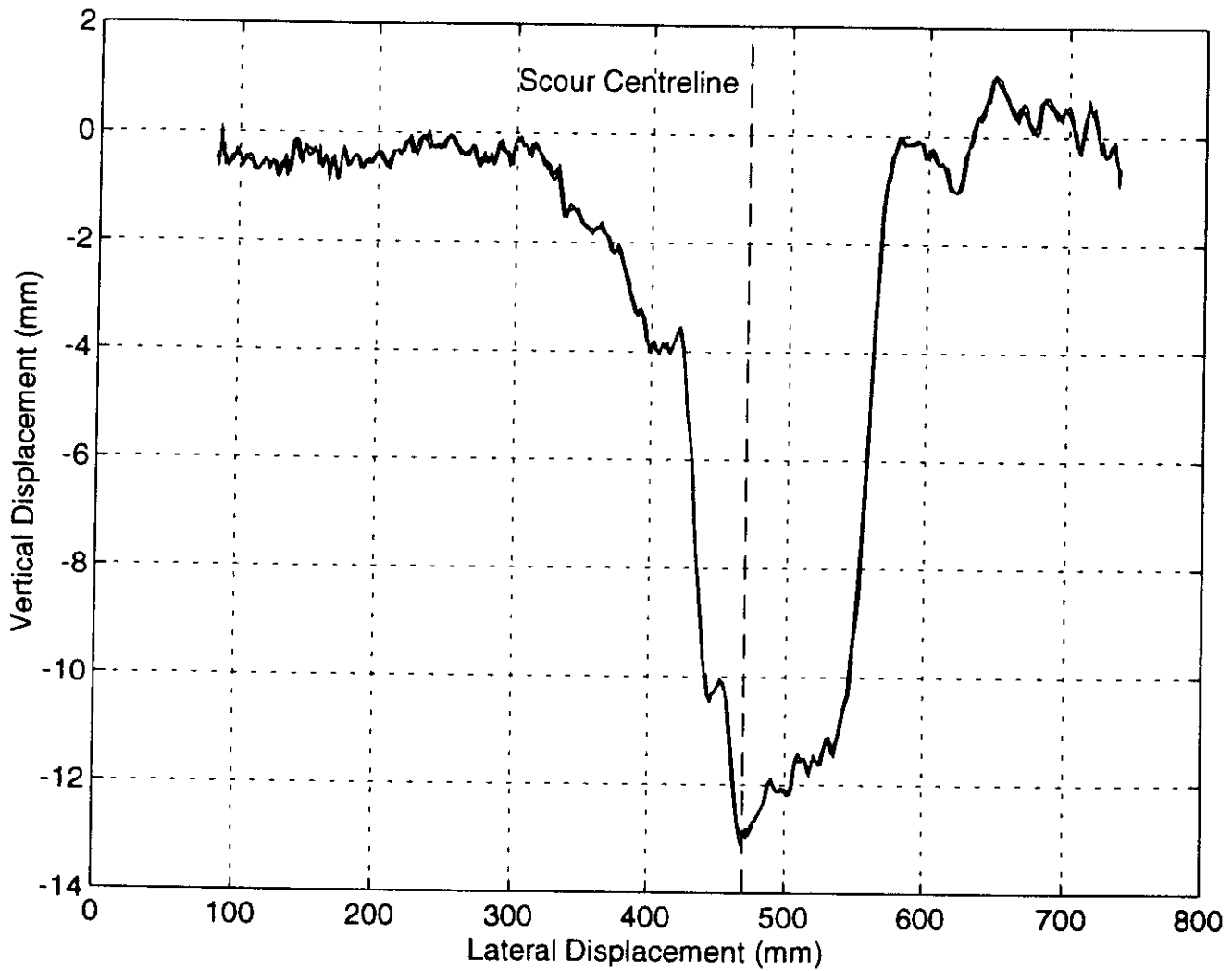




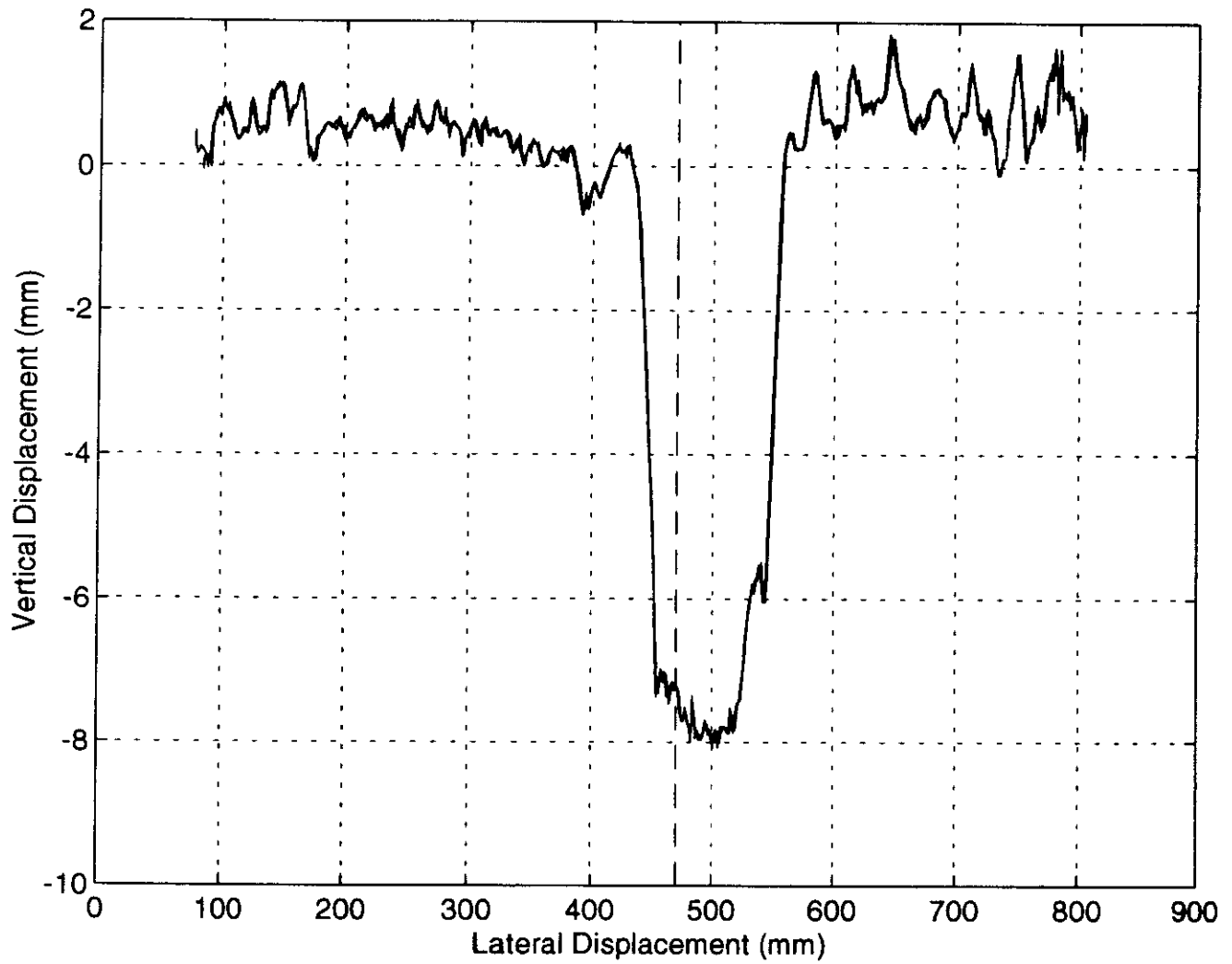




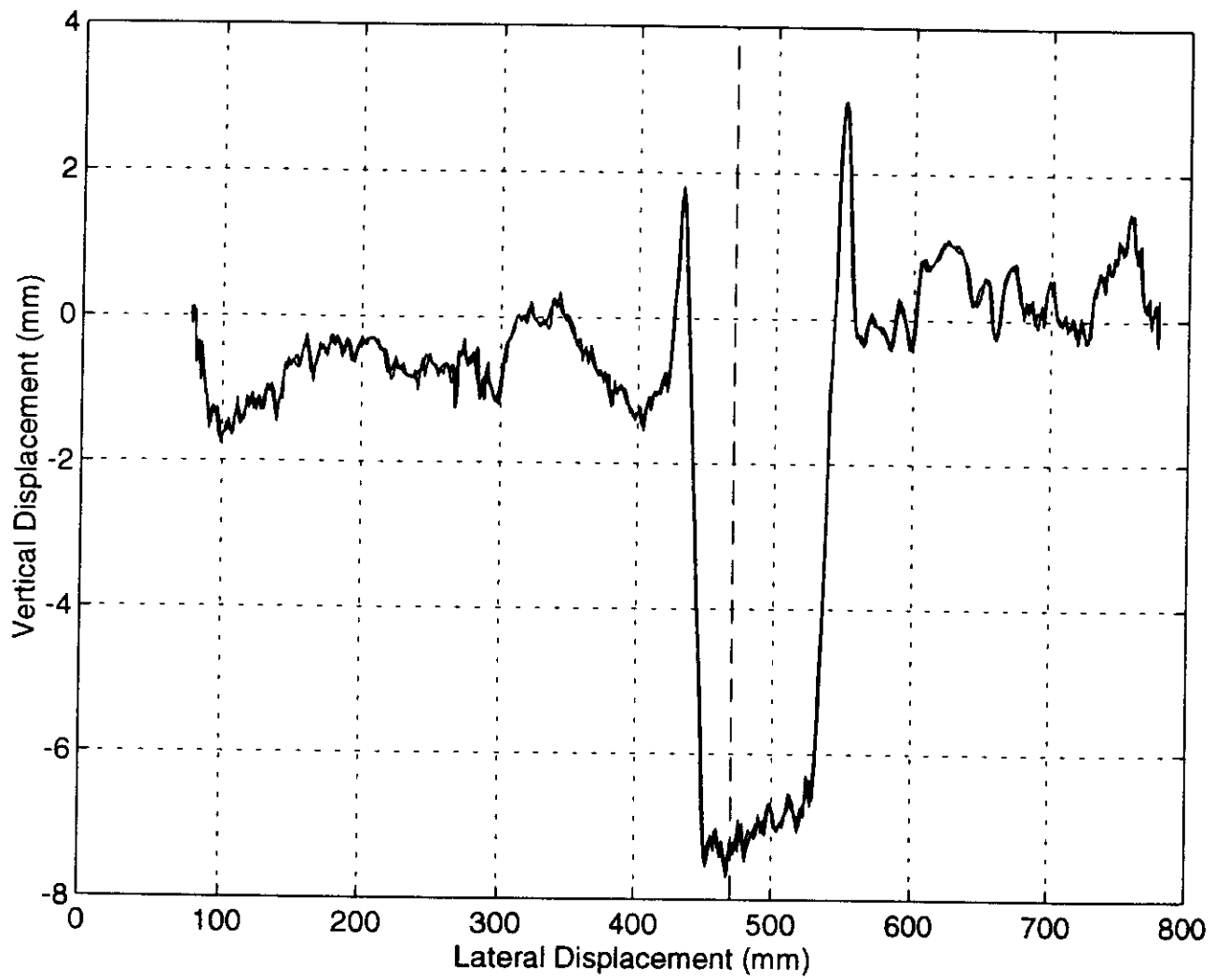




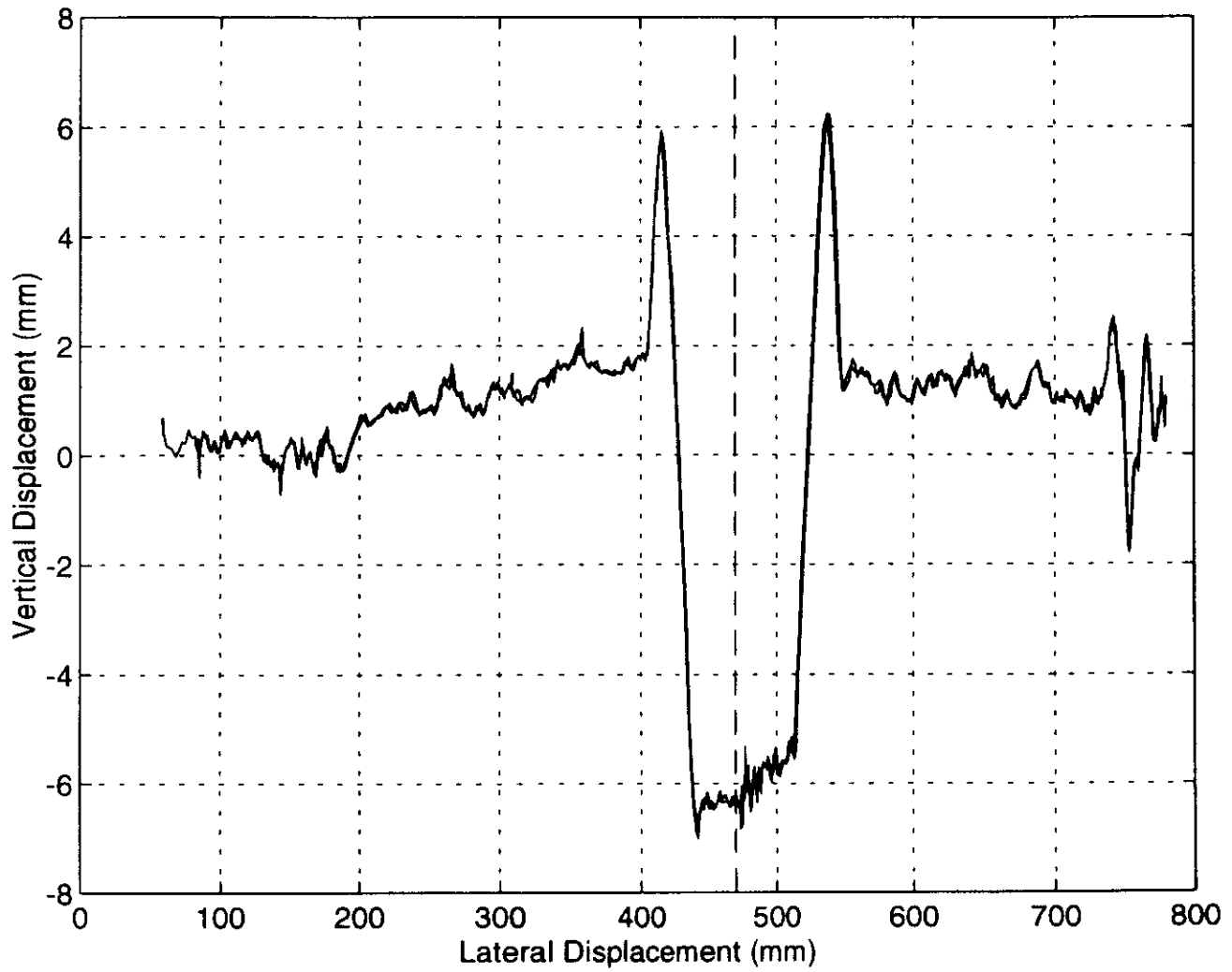
Surface Profile, Y=85 mm (Initial Keel Position)



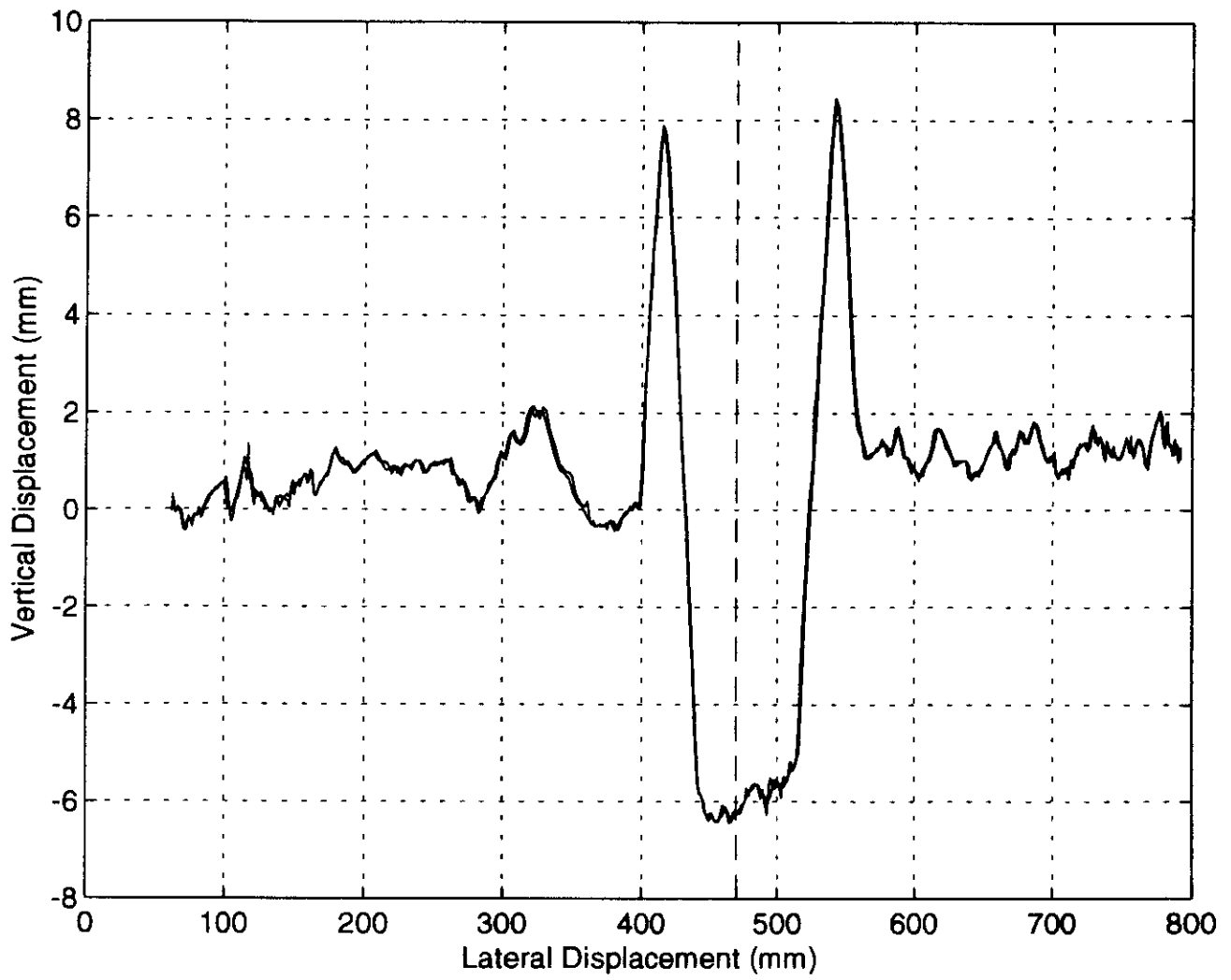
Surface Profile, Y=135 mm



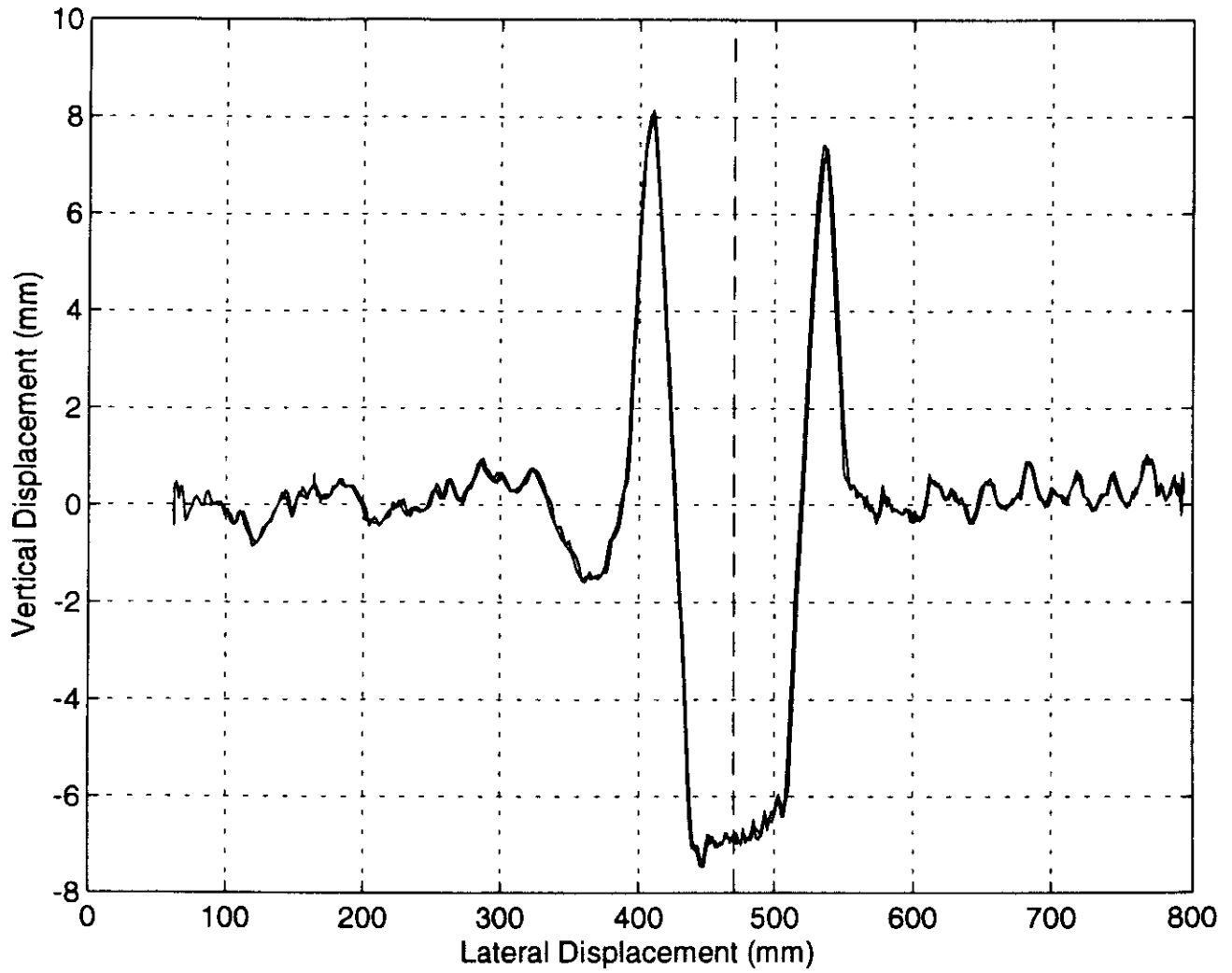
Surface Profile, Y=185 mm



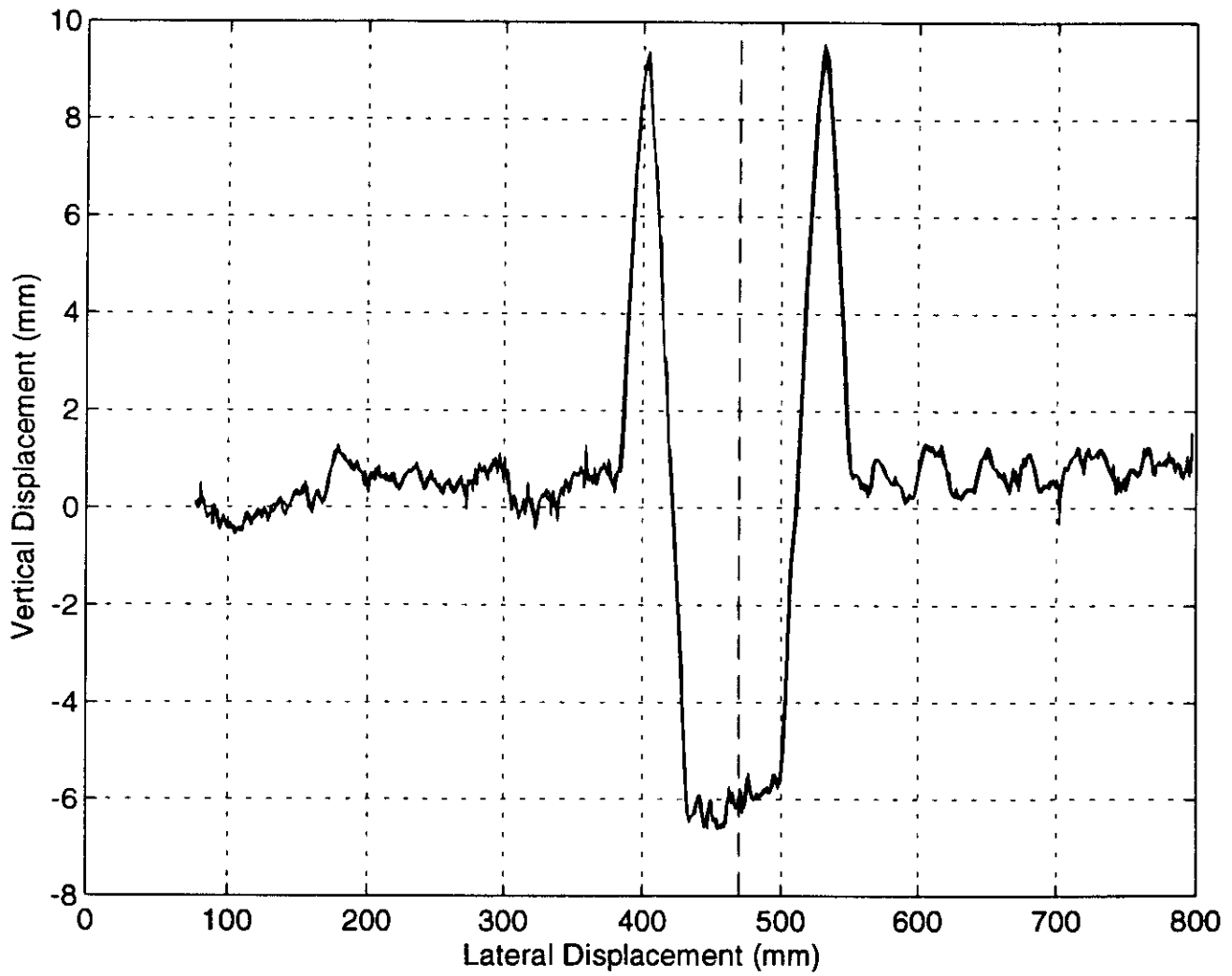
Surface Profile, Y=235 mm



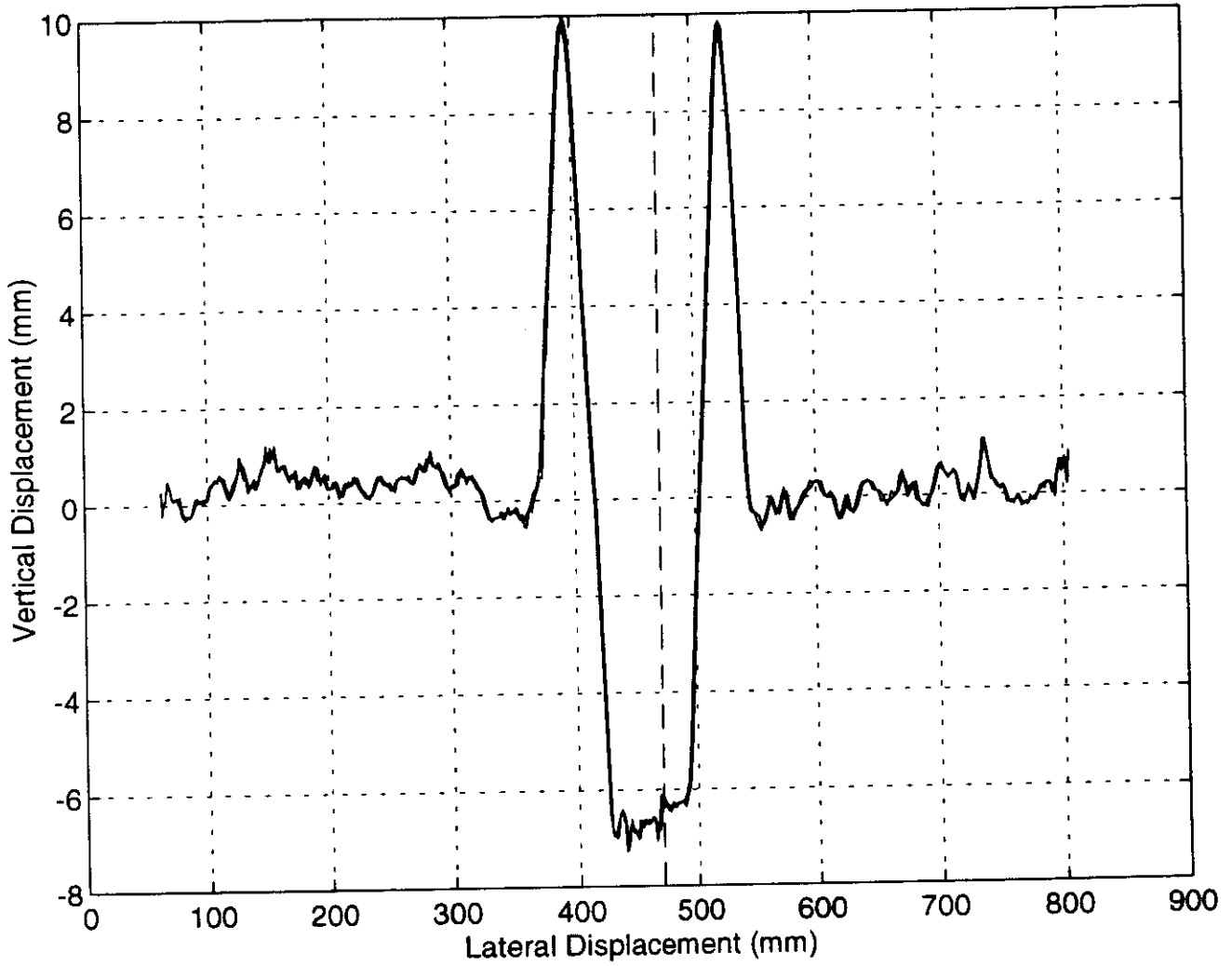
Surface Profile, Y=285 mm



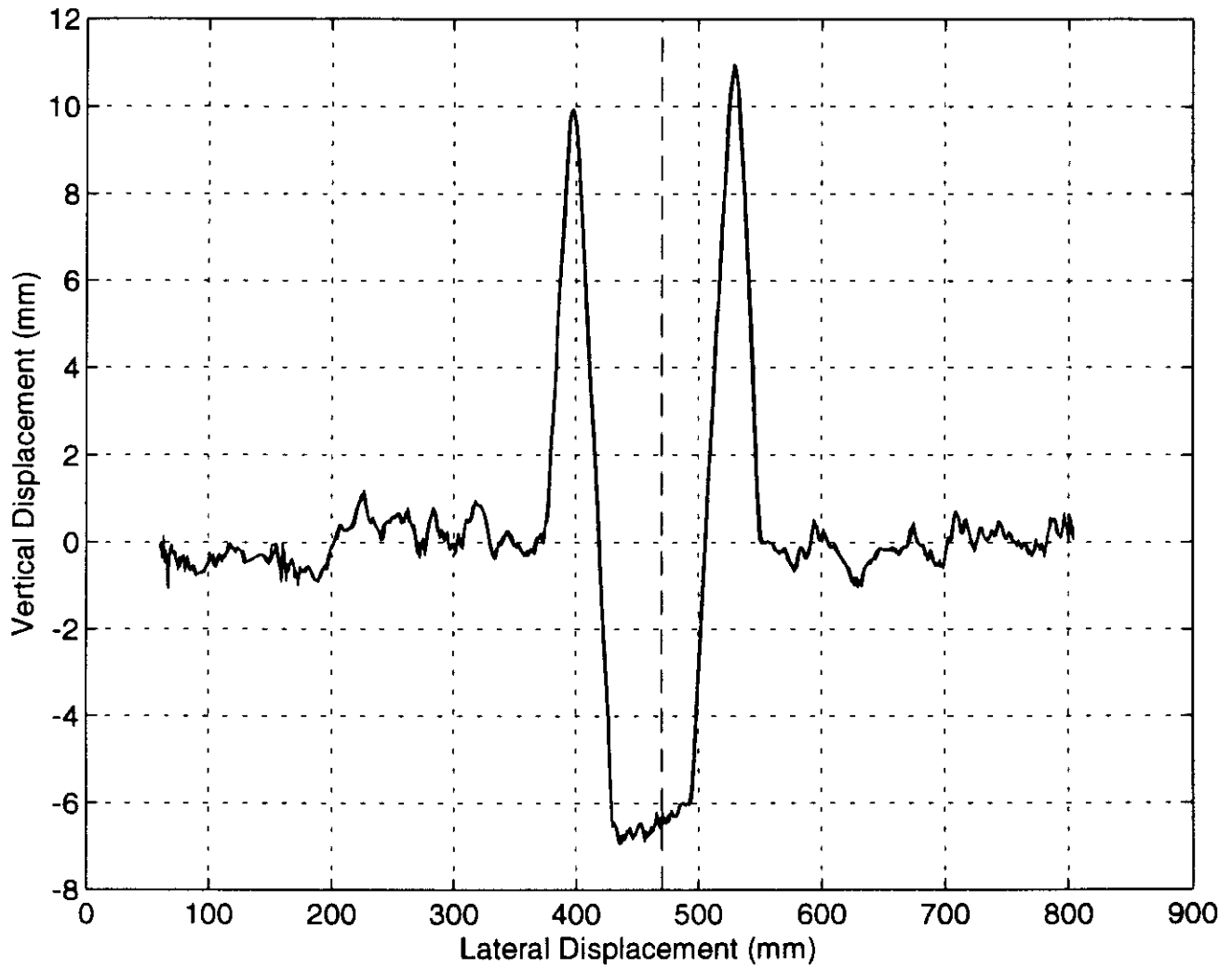
Surface Profile, Y=335 mm



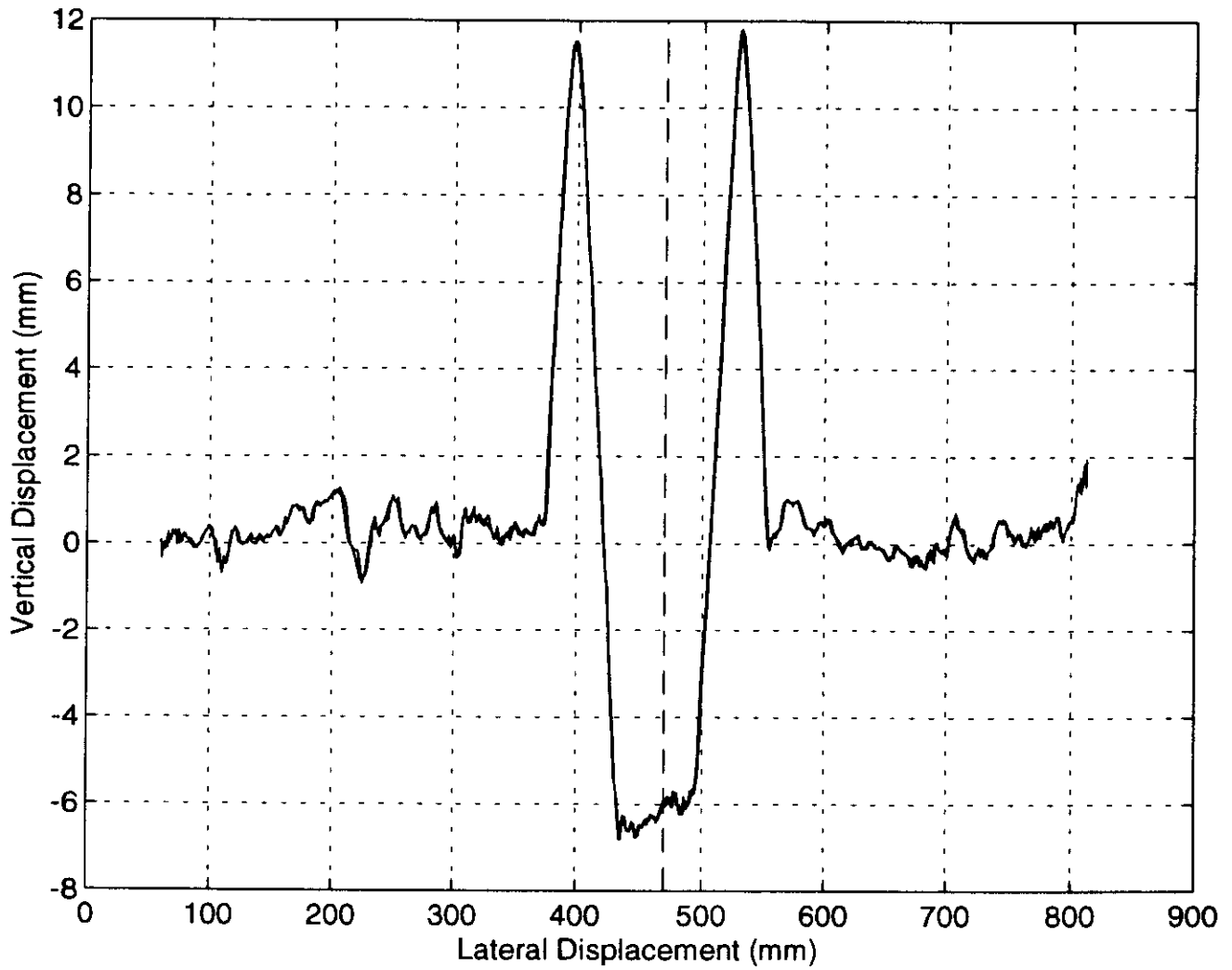
Surface Profile, Y=385 mm



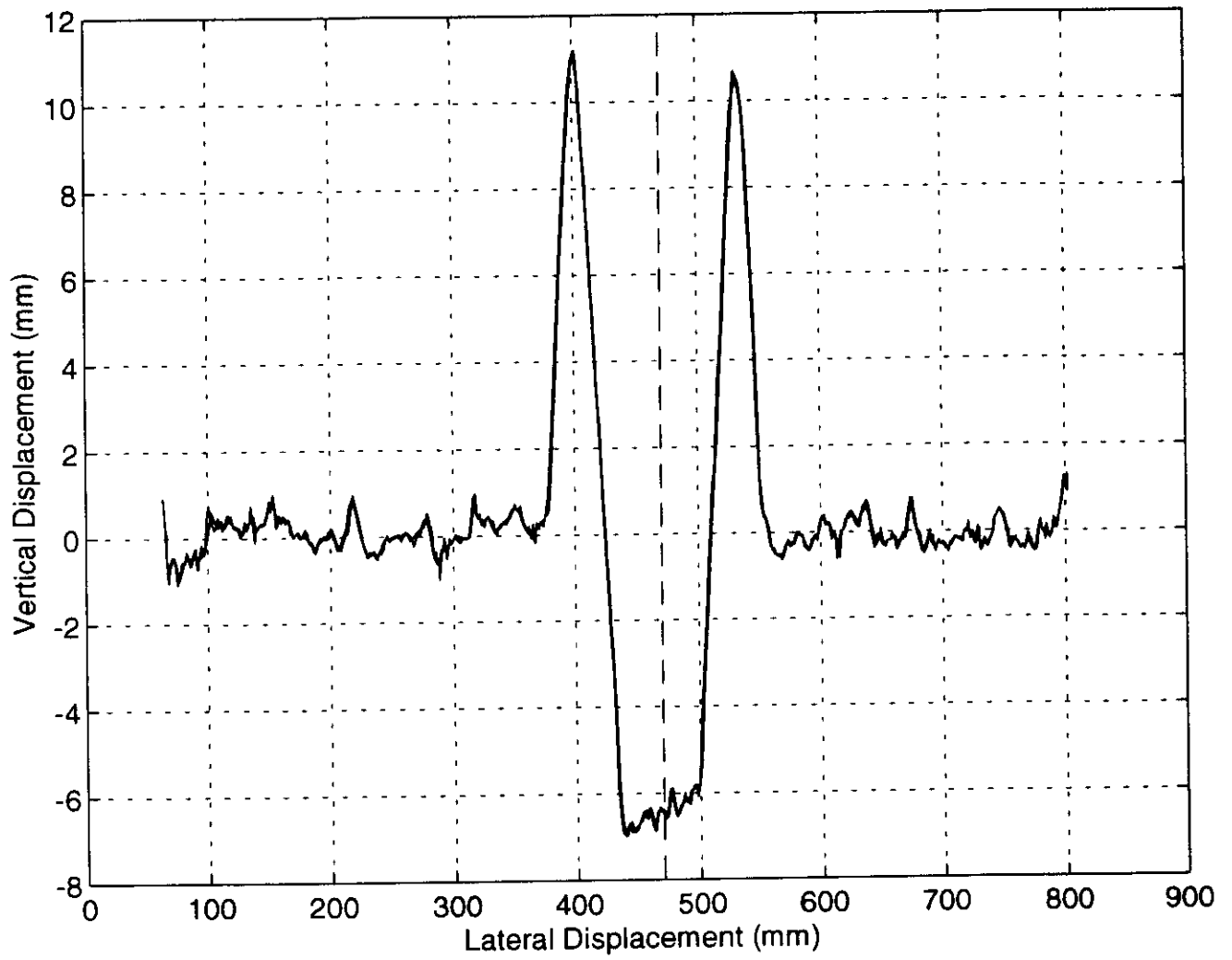
Surface Profile, Y=435 mm



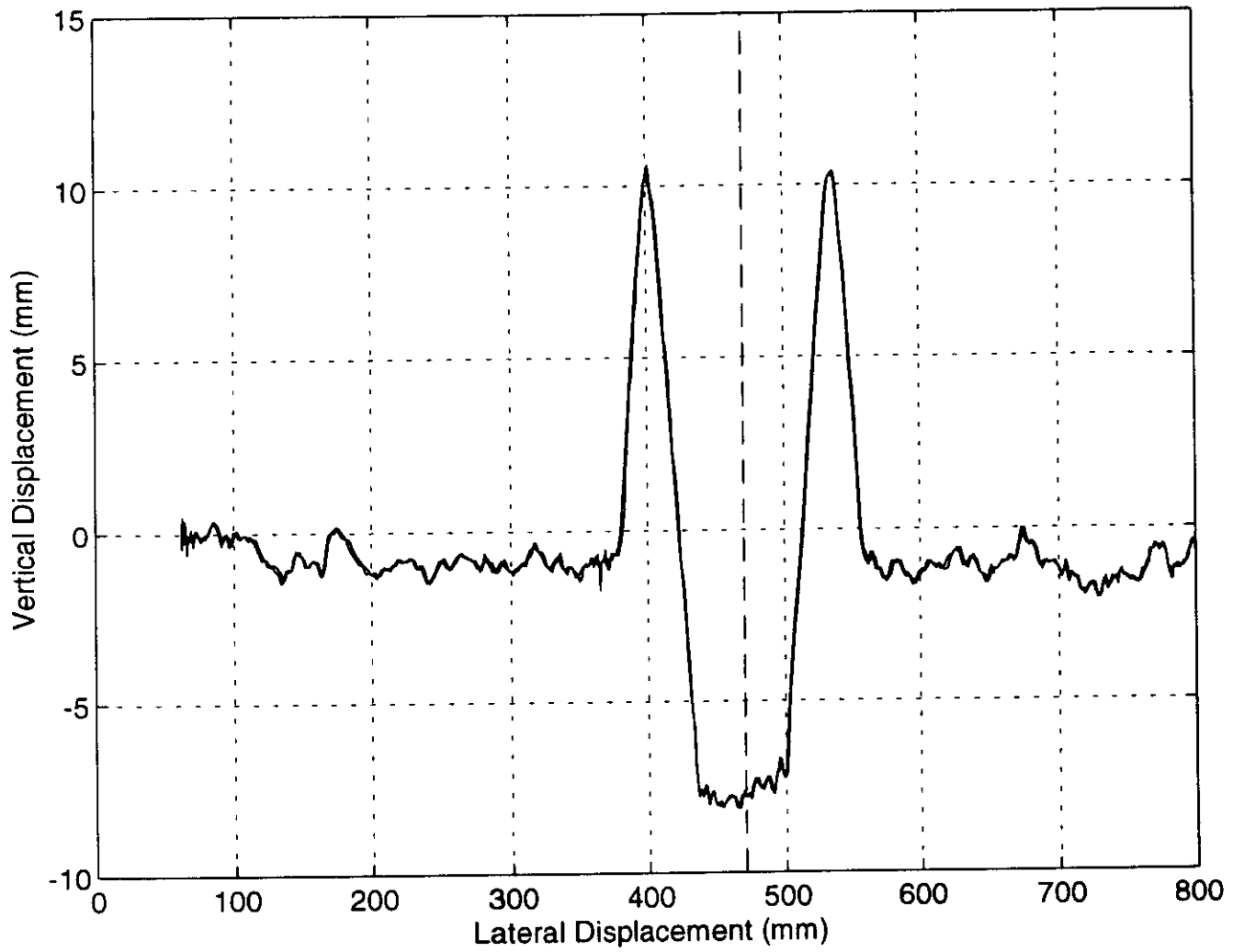
Surface Profile, Y=485 mm



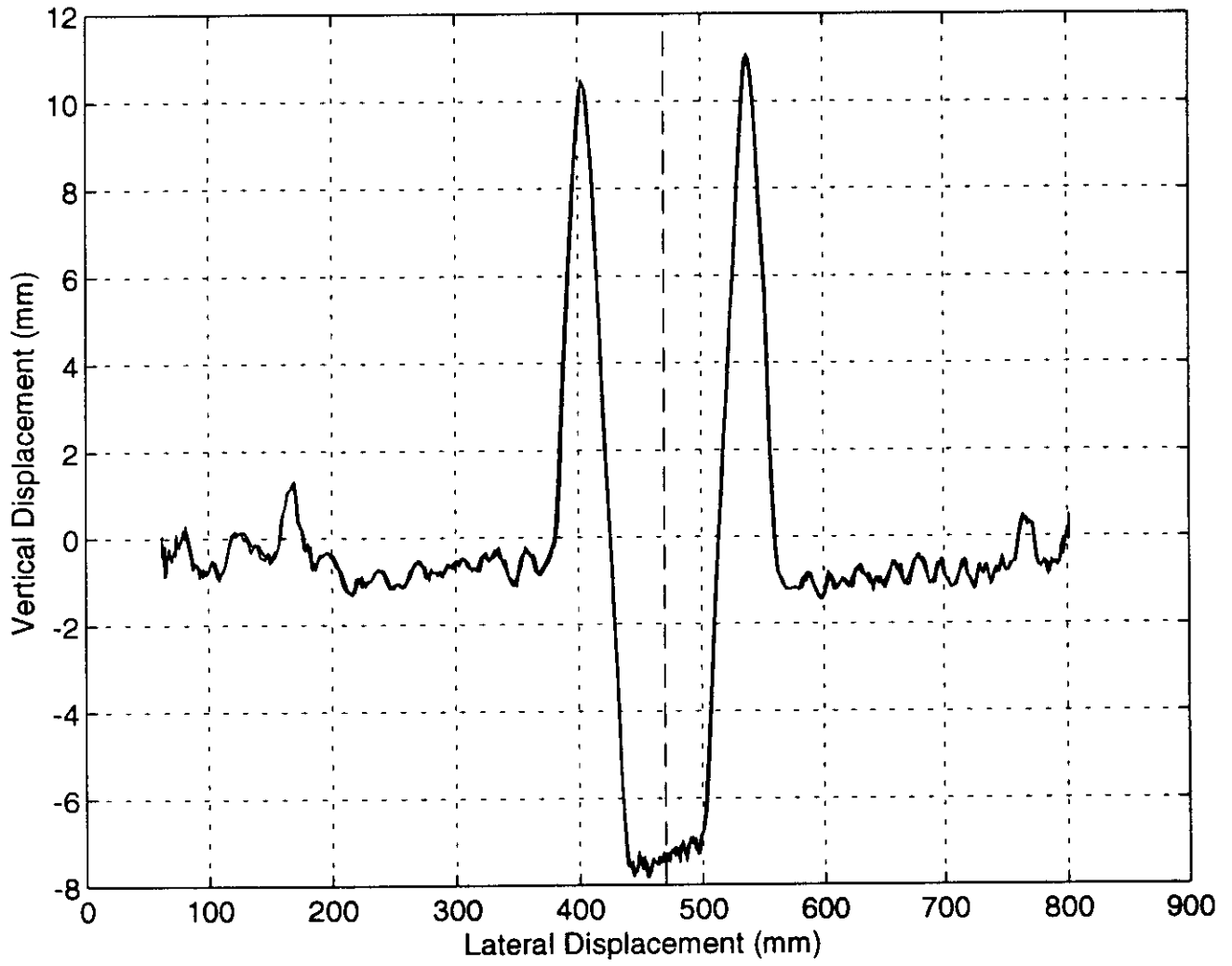
Surface Profile, Y=535 mm



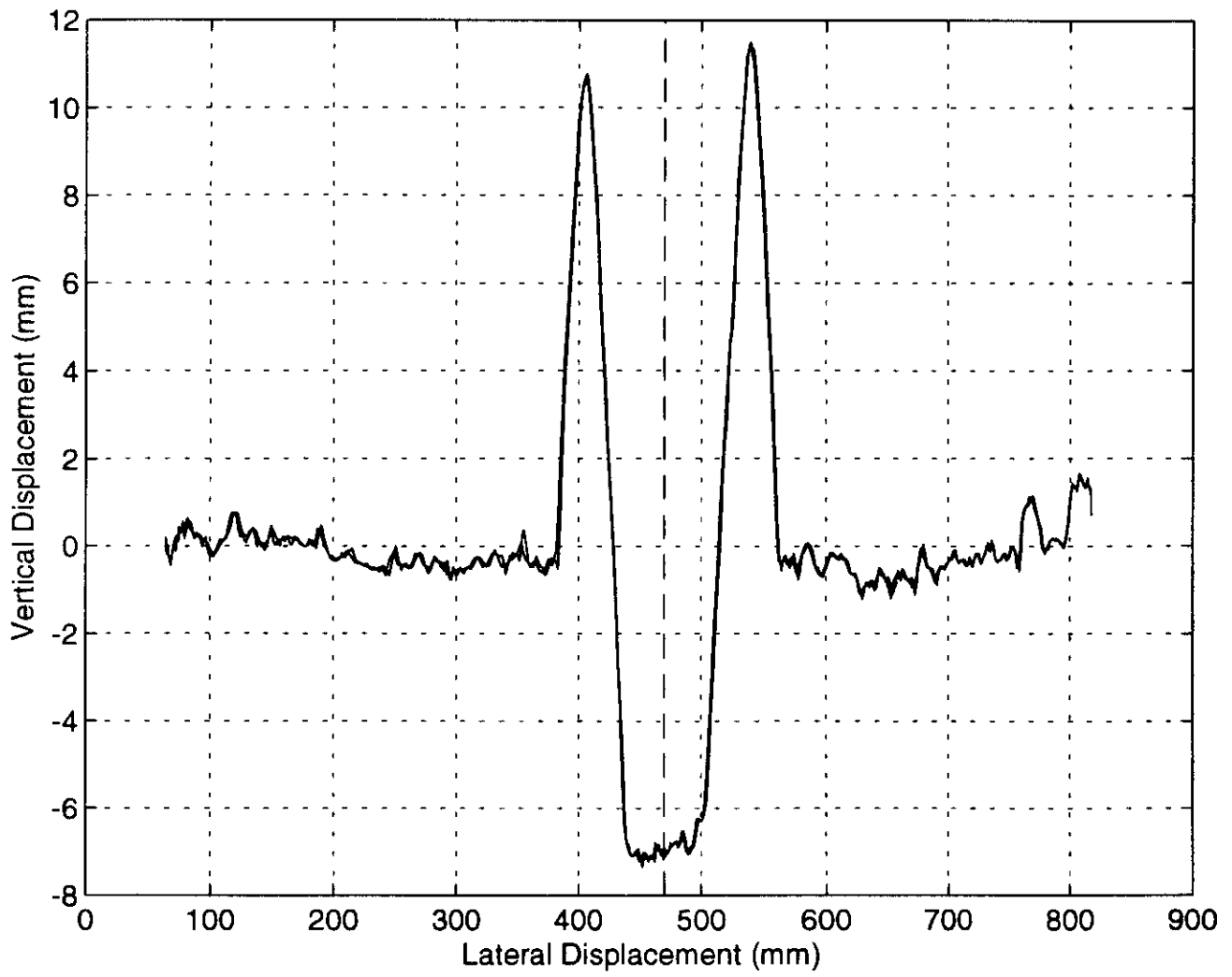
Surface Profile, Y=585 mm



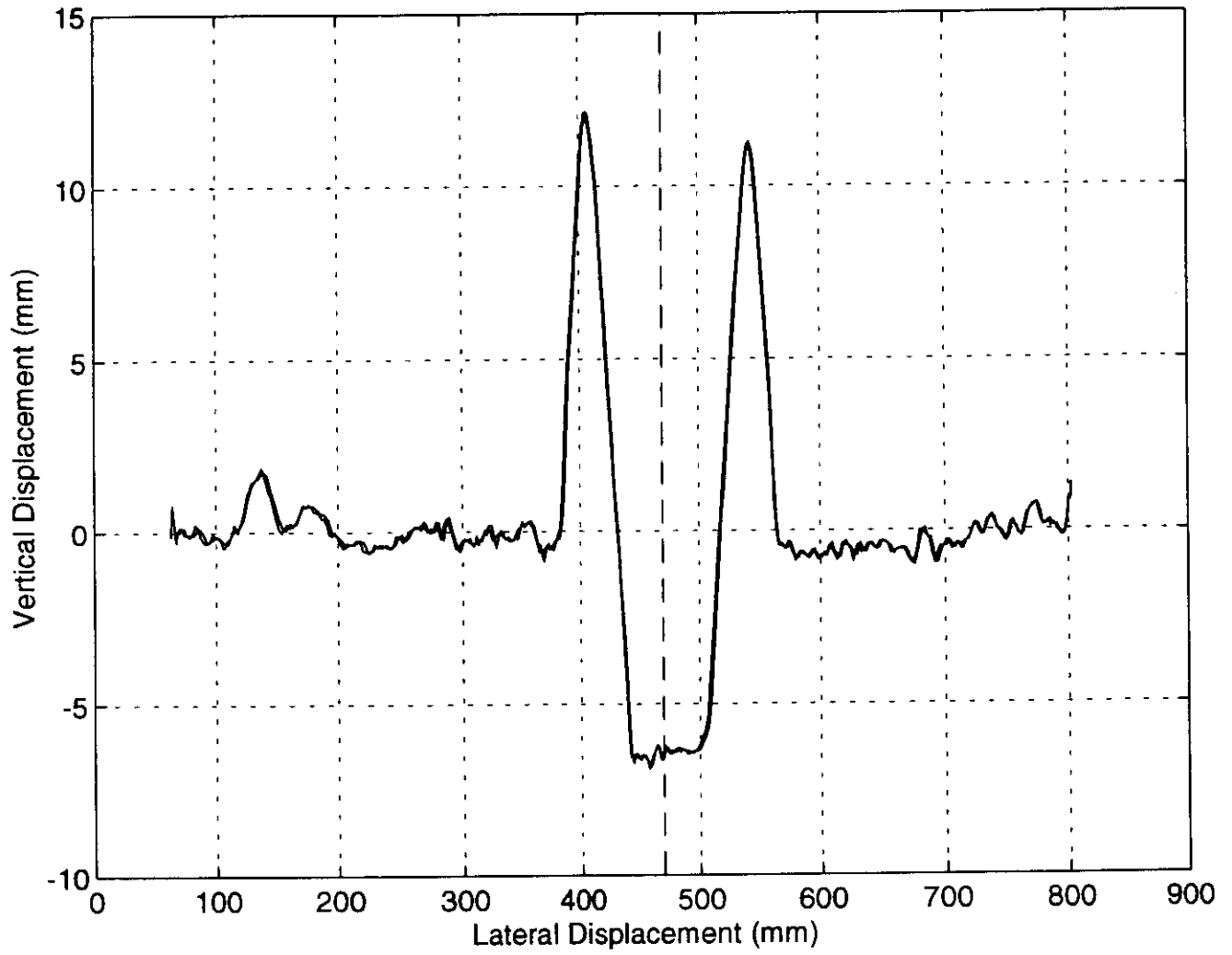
Surface Profile, Y=635 mm



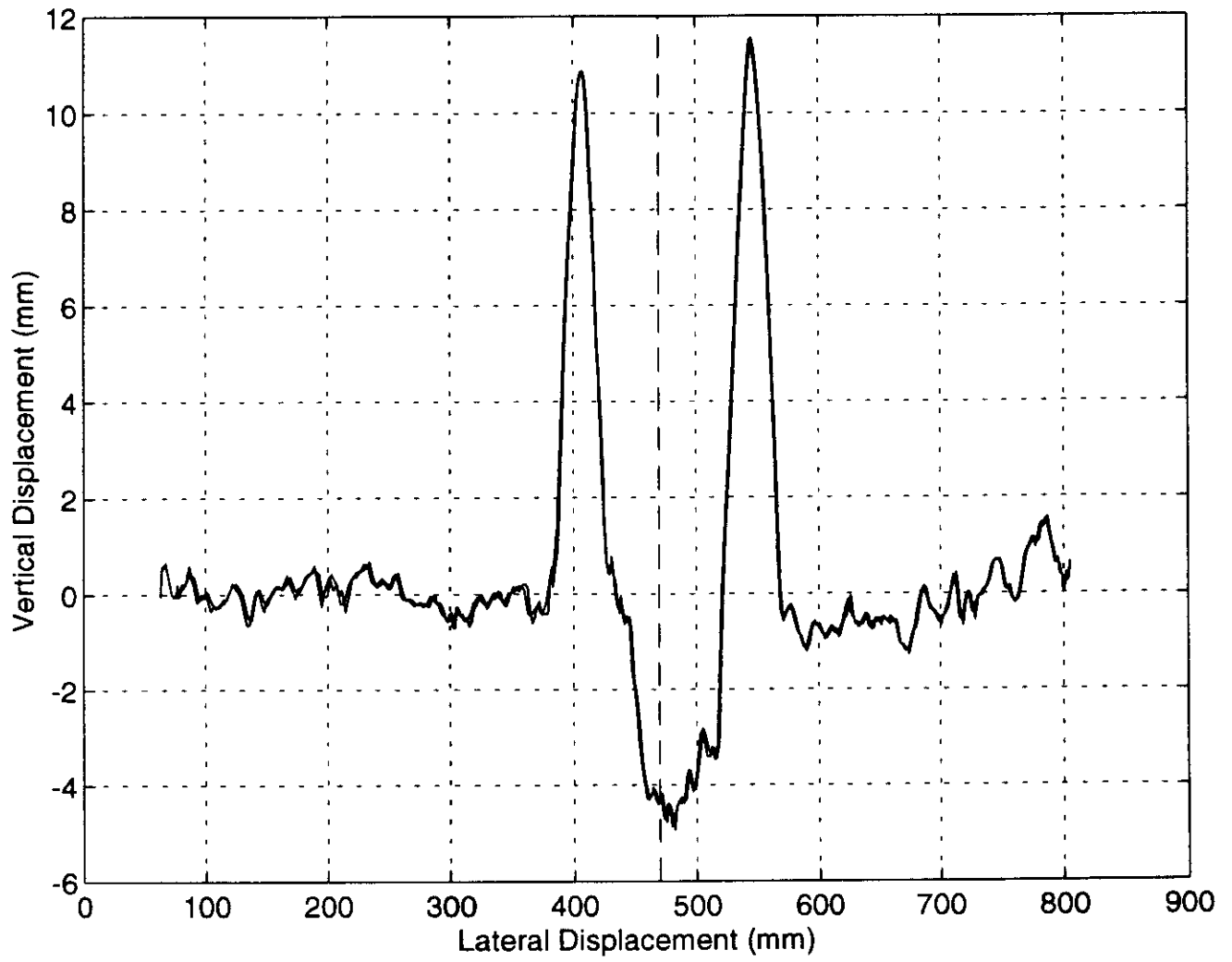
Surface Profile, Y=685 mm



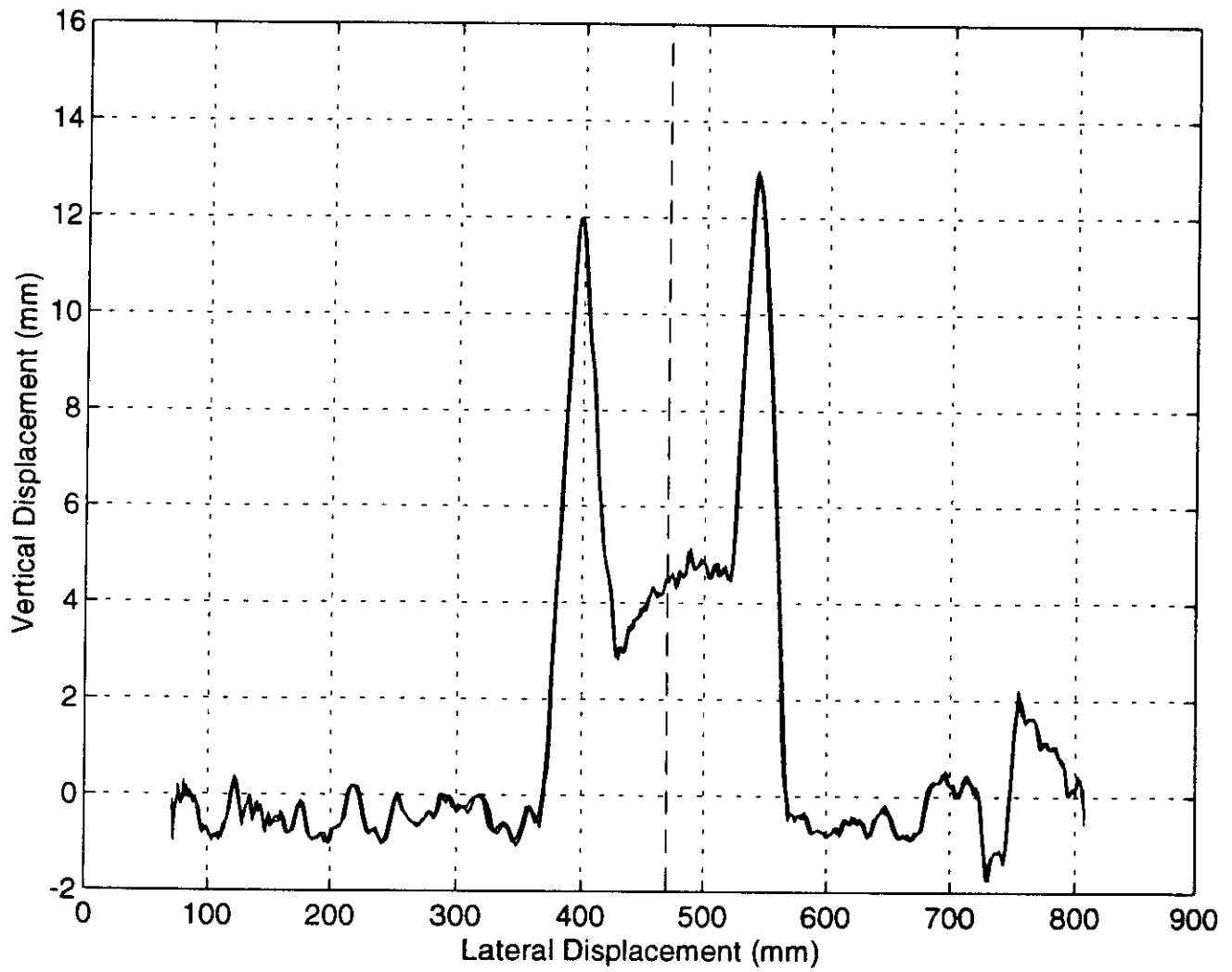
Surface Profile, Y=735 mm



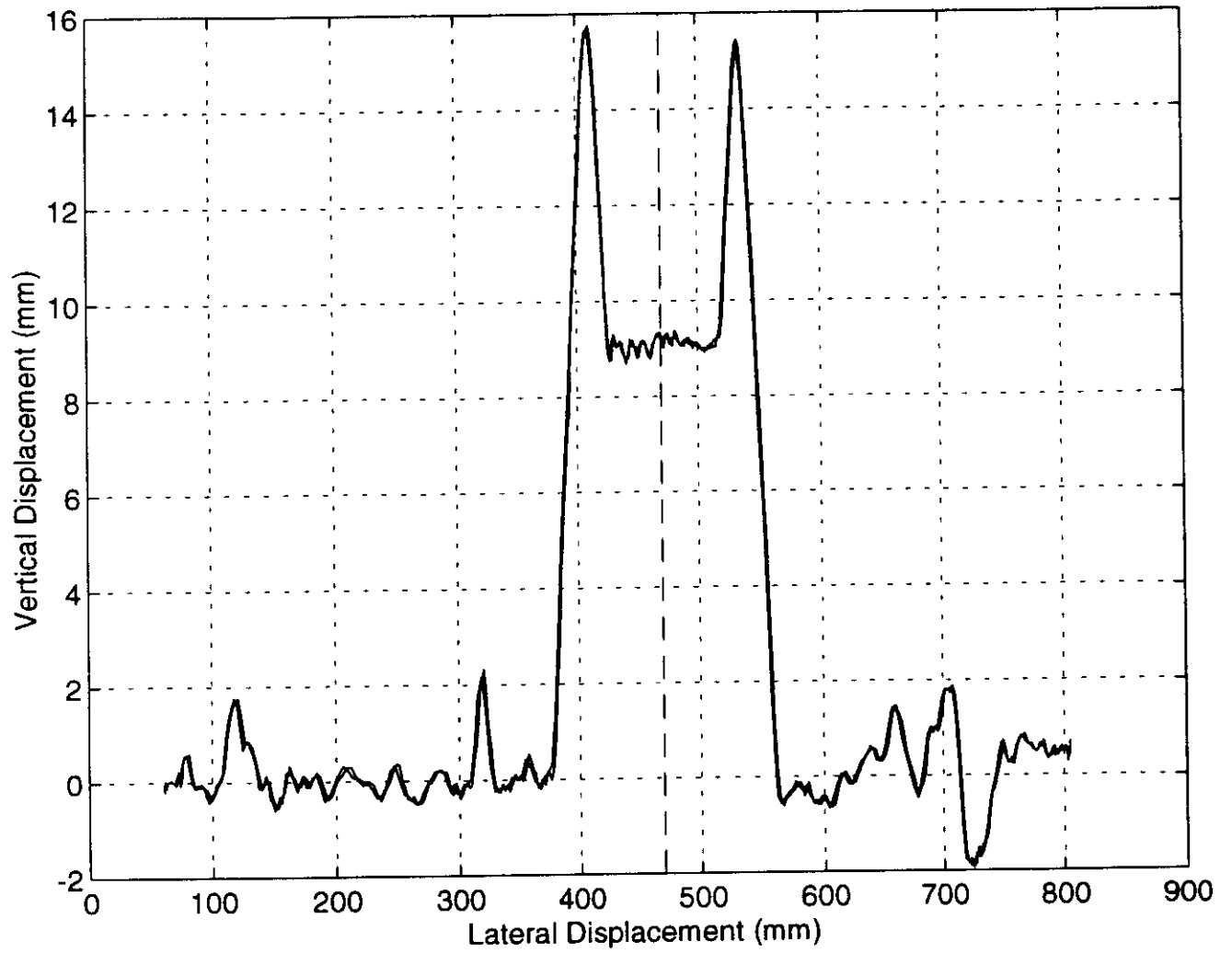
Surface Profile, Y=785 mm



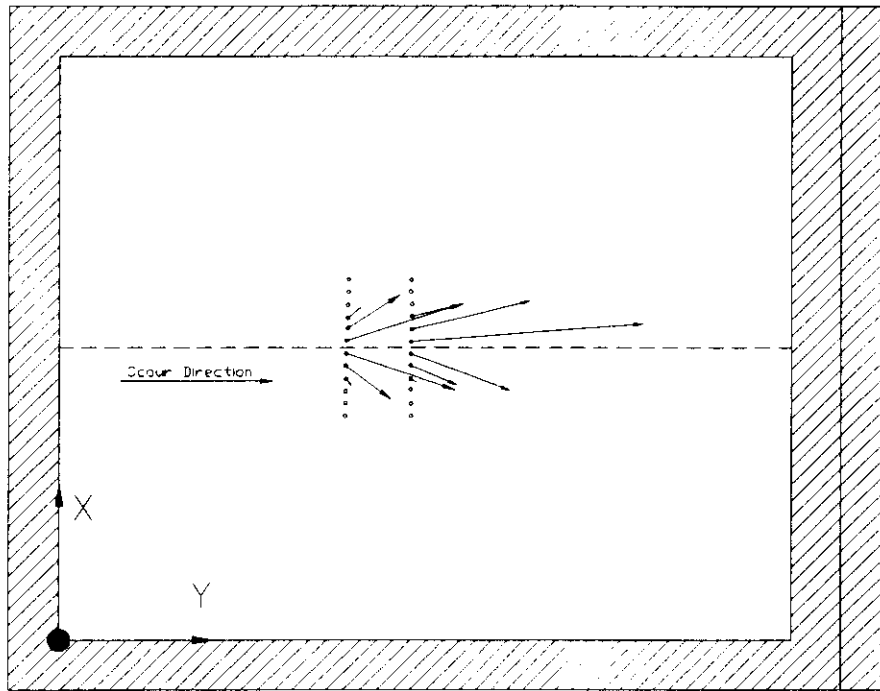
Surface Profile, Y=835 mm



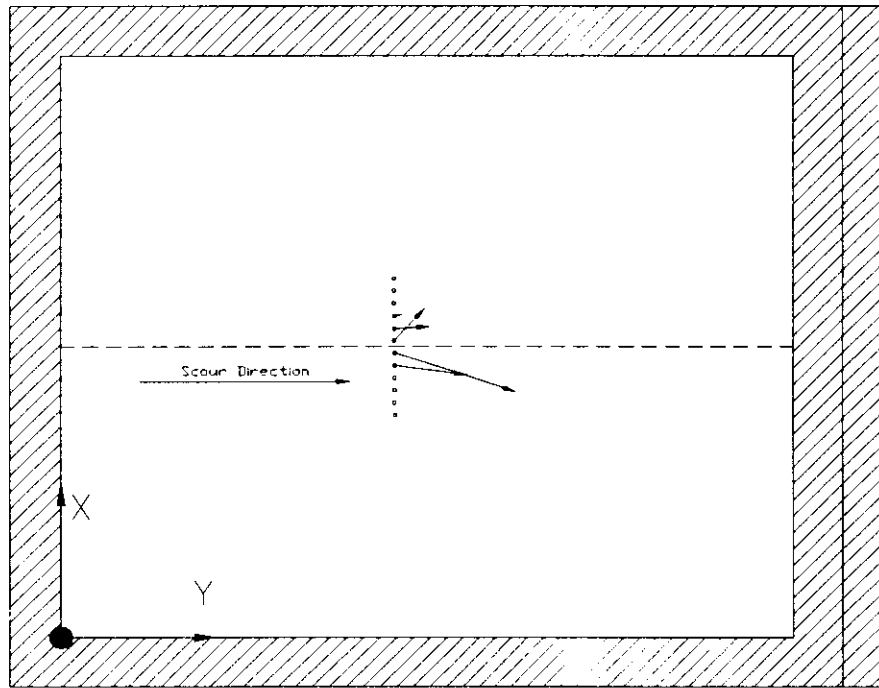
Surface Profile, Y=885 mm



Surface Profile, Y=935 mm (End of Scour)



(A)



(B)



A) Displacement Vectors - Testbed Surface  
 B) Displacement Vectors - Scour Surface

